drug-induced adverse reactions, and the efficacy of this approach was demonstrated by the discovery of a plasma biomarker of acetaminophen-induced acute hepatitis in mice.[15,16]

Here, we applied a shotgun approach based on CE-time-of-flight (TOF)-MS profiles of endogenous metabolites to identify new biomarkers of NSAID-induced gastric injury in stomach tissue extracts from rats. We then determined the correlation of concentrations of these new biomarkers in tissue extracts with that of serum concentrations.

EXPERIMENTAL SECTION

Study Design

Four week old male Sprague–Dawley (SD) rats (body weight: 65–85 g) obtained from Charles River Japan (Yokohama, Japan) were housed individually in stainless-steel wire mesh cages and allowed free access to a pellet diet (EC-2, Clea Japan, Inc., Tokyo, Japan) and filtered tap water (containing 2 ± 1 ppm free chlorine adjusted with sodium hypochlorite). Room temperature and relative humidity were maintained at 19–25 °C and 30–70% with 15 air changes/h and a 12 h light–dark cycle (lighted 7:00 a.m. to 7:00 p.m.). The animals were allowed to acclimatize for 1 week prior to entry into the study, and age and weight at the start of the study were recorded (age: 5 weeks; body weight: 120–140 g).

A total of 60 animals (n = 12 animals per group) were assigned to a control group (0.5% methylcellulose, p.o.) or one of four treatment groups: single dose aspirin (Nacalai Tesque, Kyoto, Japan) at 3 mg/kg, p.o., single dose aspirin at 300 mg/kg, p.o., single dose ibuprofen (Wako Pure Chemical Industries, Ltd., Kyoto, Japan) at 8 mg/kg, p.o., or single dose ibuprofen at 800 mg/kg, p.o. The doses used in this study were based on preliminary results (data not shown) in which the higher doses of the two compounds (300 mg/kg aspirin and 800 mg/kg ibuprofen) were demonstrated to induce gastric lesions, while the lower doses (3 mg/kg aspirin and 8 m/kg ibuprofen) were found not to induce lesions.

All experiments were carried out at Shin Nippon Biomedical Laboratories, Ltd. (Tokyo, Japan). This study was approved by the Institutional Animal Care and Use Committee of Shin Nippon Biomedical Laboratories, Ltd., and the Animal Ethical Committee of Astellas Pharma Inc. (Tokyo, Japan).

Sample Collection

Rats were anesthetized (sodium pentobarbital 32.4 mg/kg, i.p.) and exsanguinated via the abdominal aorta at 1, 5, or 24 h after dosing. Serum was collected by allowing the blood to clot at room temperature for 20 min followed by centrifugation at 1710 × g. Immediately after exsanguination, the stomach was collected and incised along the greater curvature. The tissue was then assessed macroscopically, and the interior of the stomach was photographed. The dimensions of observed gastric ulcers were determined using analySIS software (Olympus Soft Imaging Solutions GmbH, Münster, Germany). After being photographed, the stomachs were weighed, frozen in liquid nitrogen, and stored at −70 °C until sample preparation.

Sample Preparation for CE–MS

For tissue preparation, frozen stomach tissue was plunged into ice-chilled methanol (1 mL) containing internal standards (10 μM each of methionine sulfone [Wako, Osaka, Japan], D-camphor-10-sulfonic acid [CAS; Wako], and 2-(n-morpholino)-ethanesulfonic acid [MES; Dojindo, Kumamoto, Japan]), and then water and chloroform were added. After the homogenized tissue was mixed thoroughly, the solution was centrifuged at 4600 × g for 20 min at 4 °C. A 500 μL aliquot of the upper aqueous layer was then centrifugally filtered through a Millipore 5 kDa cutoff filter to remove proteins, and the filtrate was lyophilized and dissolved in 50 μL of Milli-Q water containing reference compounds (200 μM 3-aminopyrrolidine and 200 μM trimesate).

For serum preparation, a 50 μL aliquot of serum was added to 450 μL of methanol containing internal standards (20 μM each of methionine sulfone, CAS, and MES) and mixed well. Deionized water (200 μL) and 500 μL chloroform were then added, and the solution was centrifuged at 4600 × g for 8 min at 4 °C. The upper aqueous layer (approximately 800 μL) was centrifugally filtered through a Millipore 5 kDa cutoff filter to remove proteins, and the filtrate was lyophilized and dissolved in 50 μL of Milli-Q water containing reference compounds (200 μM 3-aminopyrrolidine and 200 μM trimesate).

Metabolite Standards

All chemical standards were obtained from common commercial sources. Standards were dissolved in Milli-Q water, 0.1 M HCl, or 0.1 M NaOH to obtain 10 or 100 mM stock solutions. Working standard mixtures were prepared by diluting stock solutions with Milli-Q water just prior to injection into the CE–TOF-MS system. All chemicals used as standards were of analytical or reagent grade.

Instrumentation

All CE–TOF-MS experiments were performed using an Agilent CE capillary electrophoresis system (Agilent Technologies, Waldbronn, Germany), an Agilent G3250AA LC–MSD TOFMS system (Agilent Technologies, Palo Alto, CA, U.S.A.), an Agilent1100 isocratic HPLC pump, an Agilent G1603A CE–MS adapter kit, and an Agilent G1607A CE-Electro Spray Ionization (ESI)–MS sprayer kit. System control and data acquisition were done using the Agilent G2201AA ChemStation software for CE and Analyst QS for TOF-MS.

CE–TOF-MS Conditions for Cationic Metabolite analysis

Separations were carried out in a fused silica capillary (50 μm inner diameter ×100 cm total length) filled with 1 M formic acid as the electrolyte.[17] Approximately 3 nL of sample solution was injected at 50 mbar for 3 s, followed by application of 30 kV. Capillary temperature was maintained at 20 °C, and the sample tray was cooled below 5 °C. Methanol/water (50% [v/v]) containing 0.1 μM hexakis(2,2-difluoroethoxy)phosphazene was delivered as the sheath liquid at a flow rate of 10 μL/min. ESI–TOF-MS was operated in the positive ion mode, and capillary voltage was set at 4 kV. A flow rate of heated dry nitrogen gas (heater temperature, 300 °C) was maintained at 10 psi. In TOF-MS, the fragmenter, skimmer, and Oct RFV voltage were set at 75, 50, and 125 V, respectively. Automatic recalibration of each acquired spectrum was achieved using the masses of reference standards ([^{13}C isotopic ion of a protonated methanol dimer (2MeOH + H)]$^+$, m/z 66.0632) and ([hexakis(2,2-difluoroethoxy)phosphazene + H]$^+$, m/z 622.0290). Exact mass data were acquired at a rate of 1.5 spectra/s over a 50–1000 m/z range. Total run time, including capillary preconditioning, was 45 min.

CE–TOF-MS Conditions for Anionic Metabolite Analysis

A commercially available COSMO (+) capillary (50 μm inner diameter ×100 cm total length; Nacalai Tesque, Kyoto, Japan),[18] chemically coated with a cationic polymer, was used as the separation capillary.[19] A 50 mM ammonium acetate solution (pH 8.5) was used as electrolyte solution for CE separation.

dx.doi.org/10.1021/pr3010452 | J. Proteome Res. 2013, 12, 1399–1407

Approximately 30 nL of sample solution was injected at 50 mbar for 30 s, followed by application of −30 kV. Ammonium acetate (5 mM) in 50% methanol/water (v/v) containing 0.1 μM hexakis(2,2-difluoroethoxy) phosphazene was delivered as the sheath liquid at a flow rate of 10 μL/min. ESI−TOF-MS was conducted in the negative ion mode, with the capillary voltage set at 3.5 kV. For TOF-MS, the fragmenter, skimmer, and Oct RFV voltage were set at 100, 50, and 200 V, respectively. Automatic recalibration of each acquired spectrum was performed using reference masses of reference standards ([^{13}C isotopic ion of deprotonated acetic acid dimer $(2CH_3COOH\text{-}H)]^-$, m/z 120.03841), and ([hexakis + deprotonated acetic acid $(CH_3COOH\text{-}H)]^-$, m/z 680.03554). Other conditions were identical to those previously reported.[19] Total run time, including capillary preconditioning, was 40 min.

Table 1. Severity of Gastric Ulceration Evaluated as Area of Ulceration[a]

	control	aspirin		ibuprofen	
		3 mg/kg	300 mg/kg	8 mg/kg	800 mg/kg
1 h	ND (0/4)	ND (0/4)	ND (0/4)	ND (0/4)	ND (0/4)
5 h	ND (0/4)	ND (0/4)	2.48 ± 1.14 (4/4)	ND (0/4)	18.08 ± 18.72 (4/4)
24 h	ND (0/4)	ND (0/4)	0.08 ± 0.15 (1/4)	ND (0/4)	3.76 ± 4.33 (4/4)

[a]Data are expressed as mean + SD of the area of ulceration (mm^2). Values in parentheses are the incidence rate of animals with gastric ulceration. ND: not detected.

Data Processing for Generation of the Metabolome Differential Display

To reduce data analysis time, raw data sets were preprocessed by binning the data along the m/z axis to 0.02 m/z resolution, subtracting the baseline from each electropherogram by robust nonlinear fitting of the data to a seventh-order polynomial, and removing the noise from each electropherogram by leveling to 0 all signal intensity values that fell within 5 SD of the signal intensities from 1 to 4 min. The resulting data sets were then further binned to 1 m/z unit resolution along the m/z axis. A set of peaks was selected from each data set using a modified Douglas−Peucker algorithm, with alignment of data sets along the migration time axis as described in the text. Annotation tables for both cation and anion modes were generated based on the

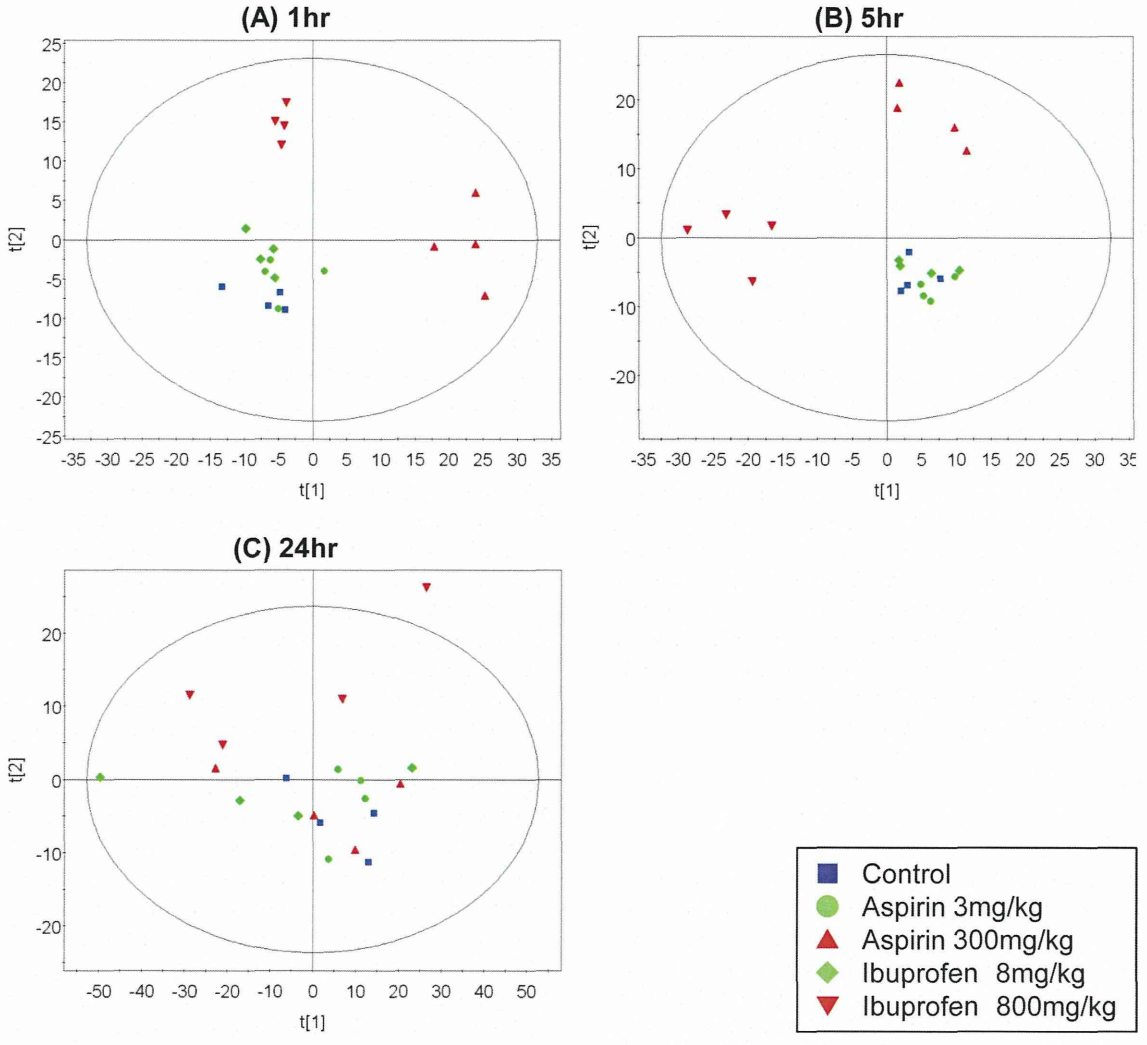

Figure 1. PCA score plots obtained from CE−MS data of stomach at 1 h (A), 5 h (B), and 24 h (C) after dosing. PCA score plot indicating discrimination between control and high-dose aspirin (300 mg/kg) or ibuprofen (800 mg/kg) at 1 and 5 h after dosing in two-dimensional PCA scores plot. This separation at 24 h after dosing was not as clear as that at 1 or 5 h postdose. Animals from the low-dose aspirin (3 mg/kg) and ibuprofen (8 mg/kg) groups showed almost the same pattern as the control group throughout the observation period.

dx.doi.org/10.1021/pr3010452 | J. Proteome Res. 2013, 12, 1399−1407

Table 2. Measured Levels of Metabolites in Stomach between Groups at 1, 5, and 24 h after Administration[a]

			aspirin		ibuprofen	
metabolite	time point	control	3 mg/kg	300 mg/kg	8 mg/kg	800 mg/kg
citrate	1 h	194 ± 21	202 ± 23	120 ± 25 (**)	202 ± 26	135 ± 39 (*)
	5 h	190 ± 18	187 ± 33	120 ± 8 (**)	172 ± 23	124 ± 19 (**)
	24 h	269 ± 75	203 ± 42	213 ± 50	175 ± 60	169 ± 52
cis-aconitate	1 h	4.7 ± 0.3	4.4 ± 0.5	2.8 ± 0.7	4.6 ± 0.6	3.6 ± 1.0
	5 h	5.4 ± 0.6	4.6 ± 1.0	3.1 ± 0.4 (**)	4.1 ± 1.0 (*)	3.1 ± 0.9 (**)
	24 h	7.7 ± 2.0	5.6 ± 0.7	5.7 ± 1.0	4.9 ± 1.6 (*)	3.7 ± 1.1 (**)
succinate	1 h	235 ± 34	252 ± 30	227 ± 28	229 ± 29	139 ± 27 (**)
	5 h	220 ± 7	231 ± 14	195 ± 8 (*)	205 ± 11	155 ± 11 (**)
	24 h	349 ± 60	323 ± 44	295 ± 80	270 ± 110	278 ± 87
o-acetyl carnitine	1 h	201 ± 14	196 ± 9	150 ± 20 (*)	206 ± 36	149 ± 29 (*)
	5 h	205 ± 9	198 ± 39	128 ± 13 (**)	164 ± 12	131 ± 25 (**)
	24 h	237 ± 41	237 ± 33	193 ± 41	195 ± 75	145 ± 39
3-hydroxybutanoic acid	1 h	565 ± 141	575 ± 110	285 ± 67 (*)	445 ± 234	188 ± 60 (**)
	5 h	690 ± 326	610 ± 211	206 ± 40 (*)	394 ± 130	404 ± 134
	24 h	596 ± 298	397 ± 217	317 ± 227	326 ± 206	175 ± 70 (*)
proline	1 h	339 ± 23	325 ± 28	274 ± 24 (**)	329 ± 25	317 ± 18
	5 h	274 ± 23	303 ± 24	247 ± 10	292 ± 22	233 ± 17 (*)
	24 h	434 ± 78	433 ± 35	428 ± 131	367 ± 134	385 ± 98
hydroxyproline	1 h	158 ± 14	130 ± 10 (*)	113 ± 8 (**)	128 ± 19 (*)	130 ± 10 (*)
	5 h	118 ± 23	128 ± 13	65 ± 11 (**)	118 ± 24	89 ± 21 (*)
	24 h	171 ± 46	154 ± 28	145 ± 36	122 ± 37	100 ± 26

[a]Mean concentration (nmol/g tissue) and standard deviation. Asterisks indicate statistically significant differences: **, $p < 0.01$; *, $p < 0.05$.

results of CE–TOF-MS analysis of standard compounds. The annotation labels were aligned to the actual data sets in a similar fashion. Arithmetic operations were applied to whole data sets on a data point-by-data point basis to highlight differences of interest. Averaging the data sets within each group allowed visualization of absolute (difference between the corresponding intensities from the averaged data sets) and relative (absolute difference divided by the larger of the two corresponding intensities) differences.

The concentrations of endogenous metabolites were imported into SIMCA-P+, version 12.0 (Umetrics, AB, Umea, Sweden). Principal components analysis (PCA) and orthogonal partial least-squares (O-PLS) were applied to get an overview of systematic variations among all observations and to identify endogenous metabolites correlated with gastric damage, respectively. To compare compound levels between groups, ANOVA and Dunnett's test were performed using GraphPad Prism, version 5.03 (GraphPad Software, San Diego, CA, U.S.A.). To analyze the correlation between the concentration of each metabolite in stomach and serum, Pearson's product-moment correlation coefficient was calculated and statistically analyzed using GraphPad Prism, version 5.03 (GraphPad Software).

RESULTS

Gastric Ulceration

The severity of gastric ulceration was presented as the ulcerative area for each group tested at one of three time points following drug administration (Table 1). No gastric ulceration was noted in control animals at any observation point following oral administration of 0.5% methylcellulose or in any animals administered either test compound at the low dose. In addition, no gastric ulceration was noted 1 h postdose in animals administered high-dose aspirin (300 mg/kg) or ibuprofen (800 mg/kg). However, by 5 h postadministration, both of the high-dose NSAID groups showed gastric ulceration, although the areas of ulceration were reduced by 97% and 79% at 24 h postdose in the aspirin and ibuprofen groups, respectively.

Metabolomic Analysis of Stomach Tissue Extracts

A total of 580 peaks were identified and quantified with metabolite standards matching the closest m/z value and normalized migration time for further statistical comparison and interpretations using the CE–TOF-MS system. (Supporting Information, Table 1) Although additional unnamed analytes were observed, we discuss only identified metabolites in the present study. As presented in Figure 1, clear separation was detected between control and high-dose aspirin (300 mg/kg) or ibuprofen (800 mg/kg) at 1 and 5 h after dosing in the two-dimensional PCA scores plot. This separation at 24 h after dosing was not as clear as at 1 or 5 h postdosing. The animals in the low-dose aspirin (3 mg/kg) and ibuprofen (8 mg/kg) groups showed almost the same pattern as that in the control group throughout the observation period. These findings suggest that these separations reflected the induction and recovery of gastric ulceration as observed in the pathological study.

Statistical analysis of quantitative differences between groups showed decreases in the levels of citrate, *cis*-aconitate, succinate, *o*-acetylcarnitine, and 3-hydroxybutanoic acid. In addition to these, decreases were also observed in proline and hydroxyproline levels in the stomach tissue extracts (Table 2 and Supporting Information, Figure 1). The selected CE–TOF-MS ion electropherograms of these metabolites are shown in Figure 2.

We superimposed metabolite concentrations changes from stomach tissue extracts on metabolic pathway maps, including those for the tricarboxylic acid cycle (TCA) cycle, β-oxidization, and glycolysis. The concentration of some metabolites in these pathways was too low for accurate detection by CE–TOF-MS, and changes in them could not be detected. While we noted suppression of the TCA cycle and β-oxidization on administration of NSAIDs, glycolysis—the upper stream of the TCA cycle—was unaffected (Figure 3).

dx.doi.org/10.1021/pr3010452 | J. Proteome Res. 2013, 12, 1399–1407

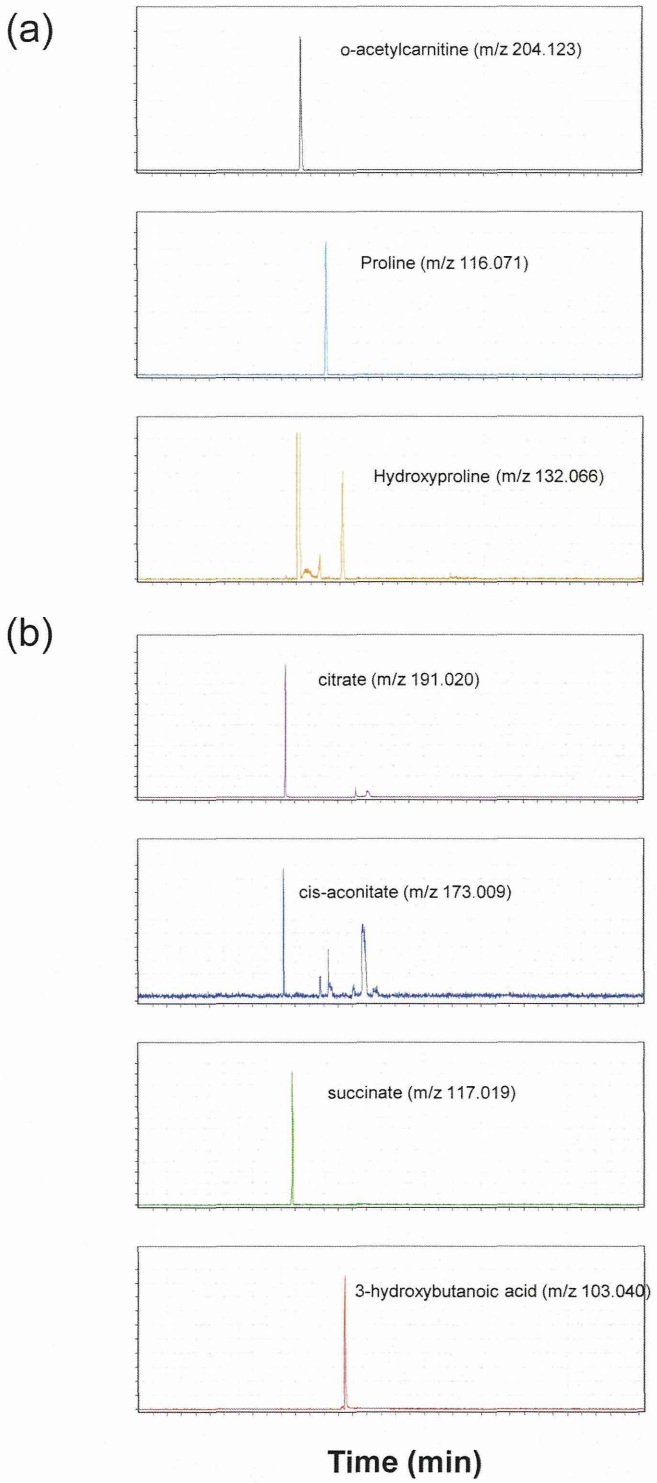

Figure 2. Selected CE–TOF-MS ion electropherograms for the stomach tissue of cationic (a) and aniomic (b) metabolites.

Metabolomic Analysis of Serum

CE–TOF-MS was used to identify and quantify 580 peaks with metabolite standards matching the closest m/z value and normalized migration time for further statistical comparison and interpretation (Supporting Information, Table 1). Although additional unnamed analytes were observed, we discussed only identified metabolites in the present study. As presented in Figure 4, clear separation was detected between control and high-dose aspirin (300 mg/kg) or ibuprofen (800 mg/kg) at 1 and 5 h after dosing in the two-dimensional PCA scores plot. Findings for quantified serum levels of these metabolites in each group at 1, 5, and 24 h after administration are presented in Table 3 and Supporting Information, Figure 2. Decreases in serum levels of *cis*-aconitate, succinate, *o*-acetyl carnitine, 3-hydroxybutanoic acid proline, and hydroxyproline levels were observed, with similar changes noted in stomach tissue extracts. In contrast, no changes were noted in serum citrate concentration.

We also assessed the correlation between concentrations of each metabolite in stomach tissue extracts and serum (Table 3). Results showed that the serum levels of each metabolite except succinate were significantly correlated with the concentrations in stomach tissue extracts.

■ DISCUSSION

Here, to identify candidate biomarkers of NSAID-induced gastric injury, we applied the metabolome differential display method based on CE–MS to a rat model of gastric ulcer induced by NSAIDs. We identified four new candidate biomarkers in the stomach which reflect this ulceration and can be detected by changes in their serum levels. Given that no biomarkers of NSAID-induced gastric ulceration in serum have yet been identified, these findings should be useful for monitoring NSAID-induced tissue damage in serum. A monitoring method using these biomarker candidates is expected to replace the current invasive practice of endoscopy.

NSAIDs, such as aspirin and ibuprofen, are among the most frequently prescribed drugs available and are commonly prescribed as analgesic, antipyretic, and anti-inflammatory drugs. Despite their widespread use, however, all NSAIDs are associated with an increased risk of gastric mucosal ulceration and hemorrhage. Given that such adverse effects are often asymptomatic and detectable only by gastric endoscopy, gastric injury associated with NSAID use can progress to life-threatening gastric ulceration and bleeding prior to detection.[1]

Administration of NSAIDs at doses that induced gastric injury in rats was associated with decreases in levels of citrate, *cis*-aconitate, succinate, *o*-acetyl carnitine, 3-hydroxy butanoic acid, proline, and hydroxyproline in stomach tissue extracts compared with tissue extracts collected from vehicle-treated control animals. Plotting these metabolite changes on metabolic pathway maps demonstrated that two events were associated with NSAID-induced gastric injury: (1) hyperactivity of collagenase in the stomach and (2) decreases in levels of citrate, *cis*-aconitate, and succinate as indications of altered TCA cycle activity, and in levels of *o*-acetyl carnitine and 3-hydroxybutanoic acid as indications of an altered acyl-carnitine pathway, both of which are mitochondrial pathways and suggest depressed mitochondrial function.

NSAIDs have been reported to induce the opening of mitochondrial permeability transition pores,[7] which in turn induces the uncoupling of oxidative phosphorylation, increases resting state respiration, and disrupts mitochondrial transmembrane potential.[20−25] These changes in mitochondrial energy production induced by NSAIDs are thought to play an important role in the induction of tissue damage.[26] In the present study, levels of citrate, *cis*-aconitate, and succinate, which are intermediates of the TCA cycle, were all decreased in stomach tissue, suggesting that the TCA cycle was inhibited by NSAIDs. However, we noted no significant changes in levels of other TCA intermediates, such as fumarate or malate, suggesting that these compounds may represent entry points for amino acid metabolism. Further, NSAID administration was associated with

dx.doi.org/10.1021/pr3010452 | J. Proteome Res. 2013, 12, 1399−1407

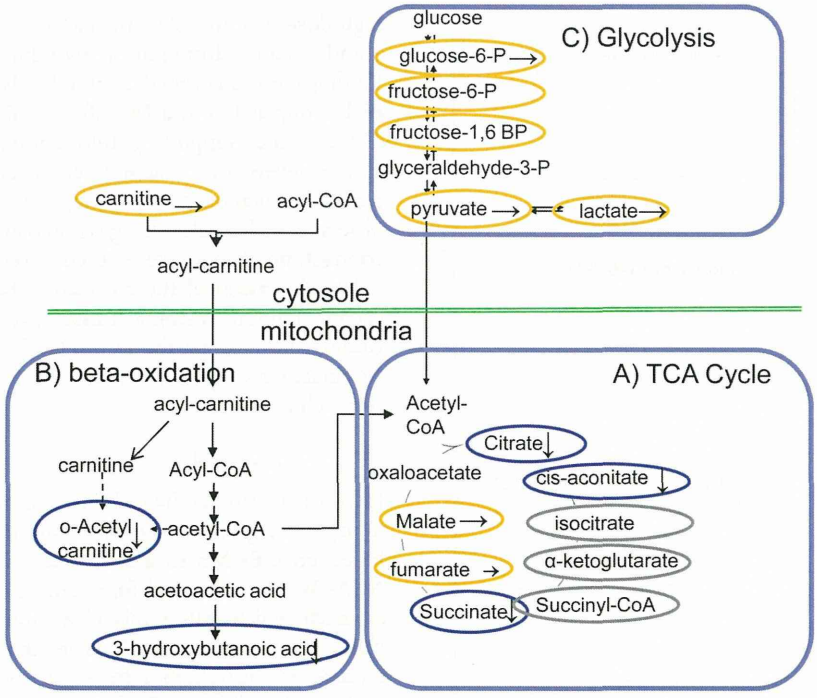

Figure 3. Observed metabolite changes in levels of stomach metabolites by a high dose of aspirin or ibuprofen mapped onto pathways. The metabolites are involved in the TCA cycle (A), β-oxidization (B), and glycolysis (C). Data were obtained by simultaneous analysis of altered levels of metabolites using CE–TOF-MS. The metabolites indicated by a blue sphere were significantly decreased by a high dose of NSAIDs. The metabolites indicated by a yellow sphere were not changed by a high dose of NSAIDs. Changes in metabolites indicated by a gray sphere could not be detected because concentrations were below detection limits.

Table 3. Measured Levels of Metabolites in Serum between Groups at 1, 5, and 24 h after Administration[a]

			aspirin		ibuprofen		
metabolite	time point	control	3 mg/kg	300 mg/kg	8 mg/kg	800 mg/kg	correlation
citrate	1 h	112 ± 5	99 ± 10	99 ± 14	112 ± 13	113 ± 8	$p < 0.01$
	5 h	116 ± 9	106 ± 10	97 ± 13	103 ± 6	100 ± 10	
	24 h	106 ± 7	96 ± 6	94 ± 18	96 ± 5	84 ± 3	
cis-aconitate	1 h	5.3 ± 0.2	5.0 ± 0.8	4.7 ± 0.5	5.4 ± 0.5	5.7 ± 0.6	$p < 0.01$
	5 h	5.8 ± 0.6	5.6 ± 0.6	4.2 ± 0.3 (**)	5.3 ± 0.5	5.1 ± 0.4	
	24 h	5.8 ± 0.9	5.4 ± 0.1	5.0 ± 0.8	5.5 ± 0.1	5.2 ± 0.3	
succinate	1 h	20 ± 2	19 ± 3	18 ± 1	18 ± 1	18 ± 2	NS
	5 h	22 ± 2	20 ± 1 (*)	24 ± 1	20 ± 1	19 ± 0 (**)	
	24 h	19 ± 1	19 ± 2	17 ± 1	18 ± 2	21 ± 3	
o-acetyl carnitine	1 h	11.4 ± 1.5	11.6 ± 1.6	11.8 ± 4.4	12.4 ± 2.1	8.8 ± 1.4	$p < 0.01$
	5 h	15.6 ± 3.9	14.3 ± 1.6	8.7 ± 1.0 (**)	9.8 ± 1.3 (*)	7.3 ± 2.6 (**)	
	24 h	15.1 ± 3.6	17.0 ± 2.6	15.1 ± 0.7	20.6 ± 8.9	8.0 ± 2.4	
3-hydroxybutanoic acid	1 h	1299 ± 241	1253 ± 130	579 ± 101 (**)	983 ± 343	466 ± 152 (*)	$p < 0.01$
	5 h	1515 ± 731	1260 ± 261	320 ± 102 (**)	880 ± 203 (*)	660 ± 213 (**)	
	24 h	971 ± 477	725 ± 235	501 ± 299	699 ± 293	311 ± 128 (*)	
proline	1 h	160 ± 18	157 ± 19	116 ± 18 (**)	137 ± 13	135 ± 14	$p < 0.01$
	5 h	150 ± 14	141 ± 10	118 ± 14 (*)	149 ± 16	104 ± 16 (**)	
	24 h	138 ± 5	153 ± 13	139 ± 26	140 ± 10	127 ± 20	
hydroxyproline	1 h	57 ± 5	51 ± 5	40 ± 8 (**)	50 ± 3	51 ± 3	$p < 0.01$
	5 h	52 ± 6	53 ± 4	28 ± 4 (**)	52 ± 6	41 ± 5 (*)	
	24 h	47 ± 5	46 ± 10	38 ± 10	43 ± 5	30 ± 8 (*)	

[a]Mean concentration (nmol/mL) and SD. Asterisks indicate statistically significant differences. **, $p < 0.01$; *, $p < 0.05$.. NS: not significant.

a decrease in 3-hydroxy butanoic acid levels from stomach tissue extracts. Given that 3-hydroxy butanoic acid is a final product and marker of fatty acid β-oxidation, decreased levels of this compound may indicate that NSAIDs also suppressed fatty acid β-oxidation.

In contrast, no changes were observed in levels of intermediates of glycolysis. Under normal conditions, pyruvate, a final product of glycolysis, is converted to acetyl-CoA, which is further incorporated into the TCA cycle for energy production. Glycolysis occurs in the cytoplasm, while the TCA cycle and fatty acid β-oxidation occur in mitochondria. The observed suppression of the TCA cycle and fatty β-oxidation with no noticeable effect on glycolysis therefore suggests an impairment of mitochondrial activity.

dx.doi.org/10.1021/pr3010452 | J. Proteome Res. 2013, 12, 1399–1407

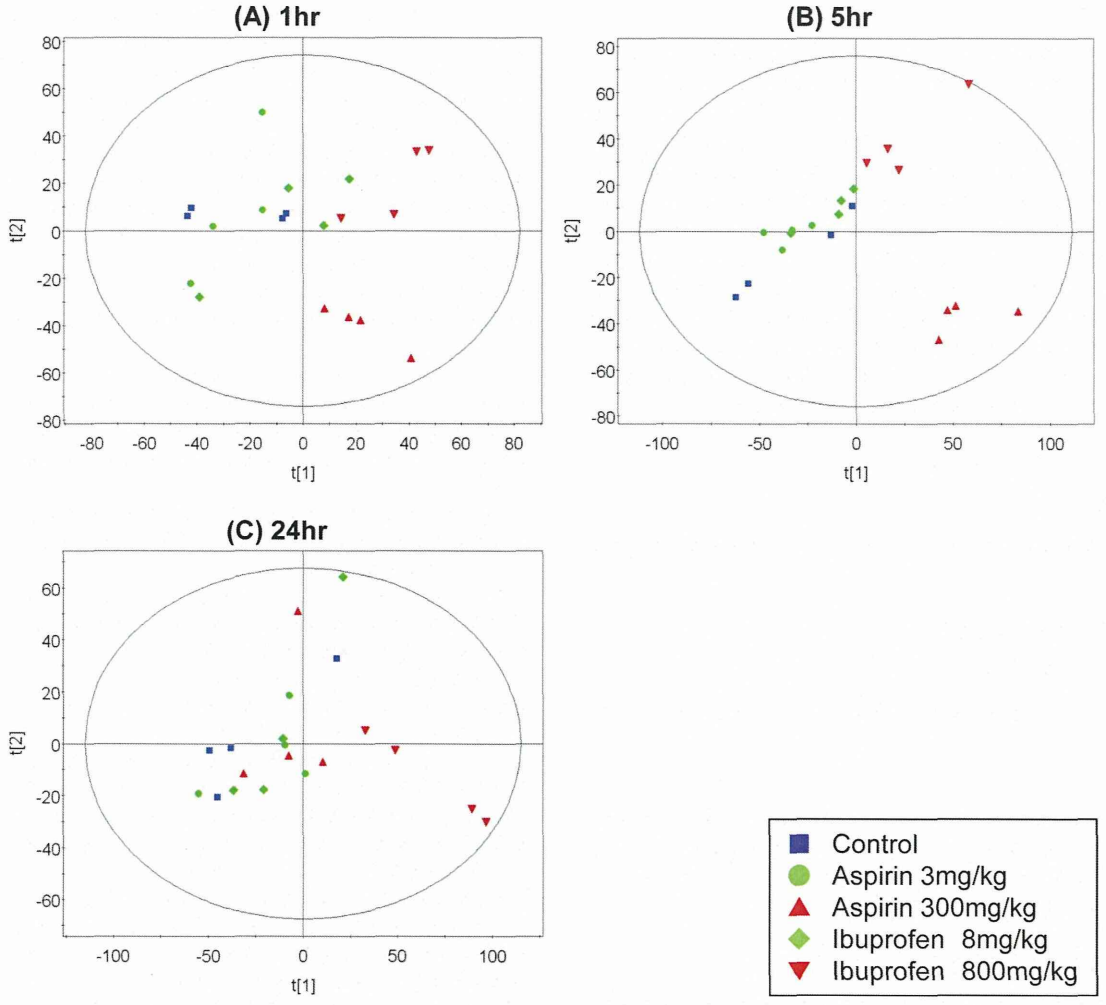

Figure 4. PCA score plots obtained from CE–MS data of serum at 1 h (A), 5 h (B), and 24 h (C) after dosing. PCA score plot indicating discrimination between the control and high-dose aspirin (300 mg/kg) or ibuprofen (800 mg/kg) groups at 1 and 5 h after dosing in two-dimensional PCA scores plot. This separation at 24 h after dosing was not as clear as that at 1 or 5 h postdose. The animals from the low-dose aspirin (3 mg/kg) or ibuprofen (8 mg/kg) groups showed almost the same pattern as the control group throughout the observation period.

Decreases in proline and hydroxyproline in stomach tissue extracts were also observed. Hydroxyproline is a modified amino acid specifically found in collagen, and proline is an amino acid which can also be found in collagen. We therefore consider that these findings are indicative of decreased collagen levels in the stomach. Indeed, previous studies have reported increased collagenase activity and a decreased amount of collagen in stomach tissue afflicted with NSAID-induced ulcers.[27] In the present study, levels of proline and hydroxyproline began to decline at 1 h after administration, with increasingly severe declines observed up to 5 h after administration and subsequent recovery at 24 h after. These changes were believed to parallel changes in gastric ulcer dimensions. While decreases in proline and hydroxyproline levels had already begun at 1 h after administration, no changes were observed at this point in the stomach. However, given that gastric ulcers were observed in all animals in both high-dose treatment groups by 5 h after administration, we surmised that gastric ulceration had indeed begun at 1 h after of administration, but that the ulcers were too small to detect on gross pathology. Accordingly, we consider that decreased levels of proline and hydroxyproline are more sensitive, earlier markers of gastric ulceration than gross pathology.

Once new biomarker candidates of gastric injury had been identified in the stomach tissue, we then assessed the levels of these same candidates in serum. Using this approach, we were able to identify noninvasively monitorable biomarker candidates of gastric ulceration induced by NSAIDs. The data showed that decreases in levels of *cis*-aconitate, *o*-acetyl carnitine, 3-hydroxybutanoic acid, proline, and hydroxyproline in stomach tissue extracts were significantly correlated with similar changes in the serum levels of these compounds, strongly suggesting that NSAID-induced changes in levels of these endogenous metabolites in the stomach are monitorable in the serum and accordingly making them favorable candidates for biomarkers of gastric injury in serum. In contrast, while decreases in citrate in the stomach were well correlated with those in serum, the degree of decrease was small and without statistical significance. A decrease in succinate in the serum was not correlated with that in the stomach. Further study is needed to clarify the mechanism of change in these biomarkers, limitation of indications, and extrapolation for application in humans. Nevertheless, these new biomarker candidates of gastric injury may prove useful for monitoring NSAID-induced tissue damage in place of the current invasive practice of endoscopy.

dx.doi.org/10.1021/pr3010452 | *J. Proteome Res.* 2013, 12, 1399–1407

CONCLUSIONS

Serum and stomach tissue extract metabolic profiles obtained using CE–MS from rats treated with NSAIDs showed drug-induced decreases in levels of citrate, *cis*-aconitate, succinate, *o*-acetyl carnitine, 3-hydroxy butanoic acid, proline, and hydroxyproline. These changes were considered due to NSAID-induced depression of mitochondrial function and activation of collagenase by lesions in the stomach. In addition, four of these changes in metabolite levels in the stomach were significantly correlated with changes in the serum. While further study is need to clarify the mechanism of change in these biomarkers, limitation of indications, and extrapolation to humans, these new non-invasive biomarker candidates of gastric injury might be useful in the monitoring of NSAID-induced tissue damage.

ASSOCIATED CONTENT

Supporting Information

This material is available free of charge via the Internet at http://pubs.acs.org.

AUTHOR INFORMATION

Corresponding Author

*E-mail: kenichiro.takeuchi@astellas.com. Telephone: +81-6-6210-7057.

Notes

The authors declare the following competing financial interest(s): This study was carried out with support from a grant from the Ministry of health, Labor and Welfare, Drug Discovery Platform Research (H20-bio-ippan-011).

ACKNOWLEDGMENTS

We are grateful to Hideaki Okatani for his technical assistance in caring for the rats and preparing samples. We also thank Dr. Marlowe Schneidkraut for his review of the manuscript and for his suggestions regarding the study. This study was carried out with support from a grant from the Ministry of health, Labor and Welfare, Drug Discovery Platform Research (H20-bioippan-011).

REFERENCES

(1) Steinmeyer, J. Pharmacological basis for the therapy of pain and inflammation with nonsteroidal anti-inflammatory drugs. *Arthritis Res.* **2000**, *2* (5), 379–85.

(2) Gabriel, S. E.; Fehring, R. A. Trends in the utilization of non-steroidal anti-inflammatory drugs in the United States, 1986–1990. *J. Clin. Epidemiol.* **1992**, *45* (9), 1041–4.

(3) Gabriel, S. E.; Jaakkimainen, L.; Bombardier, C. Risk for serious gastrointestinal complications related to use of nonsteroidal anti-inflammatory drugs. A meta-analysis. *Ann. Intern. Med.* **1991**, *115* (10), 787–96.

(4) Ishihara, T.; Tanaka, K.; Tashiro, S.; Yoshida, K.; Mizushima, T. Protective effect of rebamipide against celecoxib-induced gastric mucosal cell apoptosis. *Biochem. Pharmacol.* **2010**, *79* (11), 1622–33.

(5) Hawkey, C. J. Nonsteroidal anti-inflammatory drug gastropathy. *Gastroenterology* **2000**, *119* (2), 521–35.

(6) Sutherland, L. R.; Verhoef, M.; Wallace, J. L.; Van Rosendaal, G.; Crutcher, R.; Meddings, J. B. A simple, non-invasive marker of gastric damage: sucrose permeability. *Lancet* **1994**, *343* (8904), 998–1000.

(7) Szewczyk, A.; Wojtczak, L. Mitochondria as a pharmacological target. *Pharmacol. Rev.* **2002**, *54* (1), 101–27.

(8) Richardson, P.; Hawkey, C. J.; Stack, W. A. Proton pump inhibitors. Pharmacology and rationale for use in gastrointestinal disorders. *Drugs* **1998**, *56* (3), 307–35.

(9) Takeda, M.; Takagi, T.; Yashima, Y.; Maeno, H. Effect of a new potent H2-blocker, 3-[[[2-(diaminomethylene)amino]-4-thiazolyl]-methyl]thio]-N2-sulfamoyl propionamidine (YM-11170), on gastric secretion, ulcer formation and weight of male accessory sex organs in rats. *Arzneimittelforschung* **1982**, *32* (7), 734–7.

(10) Fiehn, O.; Kopka, J.; Dormann, P.; Altmann, T.; Trethewey, R. N.; Willmitzer, L. Metabolite profiling for plant functional genomics. *Nat. Biotechnol.* **2000**, *18* (11), 1157–61. (b) Schauer, N.; Semel, Y.; Roessner, U.; Gur, A.; Balbo, I.; Carrari, F.; Pleban, T.; Perez-Melis, A.; Bruedigam, C.; Kopka, J.; Willmitzer, L.; Zamir, D.; Fernie, A. R. Comprehensive metabolic profiling and phenotyping of interspecific introgression lines for tomato improvement. *Nat. Biotechnol.* **2006**, *24* (4), 447–54.

(11) Plumb, R.; Granger, J.; Stumpf, C.; Wilson, I. D.; Evans, J. A.; Lenz, E. M. Metabonomic analysis of mouse urine by liquid-chromatography-time of flight mass spectrometry (LC-TOFMS): detection of strain, diurnal and gender differences. *Analyst* **2003**, *128* (7), 819–23.

(12) Monton, M. R.; Soga, T. Metabolome analysis by capillary electrophoresis-mass spectrometry. *J. Chromatogr. A* **2007**, *1168* (1–2), 237–46 discussion 236.

(13) Nicholson, J. K.; Connelly, J.; Lindon, J. C.; Holmes, E. Metabonomics: a platform for studying drug toxicity and gene function. *Nat. Rev. Drug Discovery* **2002**, *1* (2), 153–61.

(14) Soga, T.; Ohashi, Y.; Ueno, Y.; Naraoka, H.; Tomita, M.; Nishioka, T. Quantitative metabolome analysis using capillary electrophoresis mass spectrometry. *J. Proteome Res.* **2003**, *2* (5), 488–94.

(15) Soga, T.; Baran, R.; Suematsu, M.; Ueno, Y.; Ikeda, S.; Sakurakawa, T.; Kakazu, Y.; Ishikawa, T.; Robert, M.; Nishioka, T.; Tomita, M. Differential metabolomics reveals ophthalmic acid as an oxidative stress biomarker indicating hepatic glutathione consumption. *J. Biol. Chem.* **2006**, *281* (24), 16768–76.

(16) Shintani, T.; Iwabuchi, T.; Soga, T.; Kato, Y.; Yamamoto, T.; Takano, N.; Hishiki, T.; Ueno, Y.; Ikeda, S.; Sakuragawa, T.; Ishikawa, K.; Goda, N.; Kitagawa, Y.; Kajimura, M.; Matsumoto, K.; Suematsu, M. Cystathionine beta-synthase as a carbon monoxide-sensitive regulator of bile excretion. *Hepatology* **2009**, *49* (1), 141–50.

(17) Soga, T.; Heiger, D. N. Amino acid analysis by capillary electrophoresis electrospray ionization mass spectrometry. *Anal. Chem.* **2000**, *72* (6), 1236–41.

(18) Katayama, H.; Ishihama, Y.; Asakawa, N. Stable cationic capillary coating with successive multiple ionic polymer layers for capillary electrophoresis. *Anal. Chem.* **1998**, *70* (24), 5272–7.

(19) Soga, T.; Igarashi, K.; Ito, C.; Mizobuchi, K.; Zimmermann, H. P.; Tomita, M. Metabolomic profiling of anionic metabolites by capillary electrophoresis mass spectrometry. *Anal. Chem.* **2009**, *81* (15), 6165–74.

(20) Petrescu, I.; Tarba, C. Uncoupling effects of diclofenac and aspirin in the perfused liver and isolated hepatic mitochondria of rat. *Biochim. Biophys. Acta* **1997**, *1318* (3), 385–94.

(21) Moreno-Sanchez, R.; Bravo, C.; Vasquez, C.; Ayala, G.; Silveira, L. H.; Martinez-Lavin, M. Inhibition and uncoupling of oxidative phosphorylation by nonsteroidal anti-inflammatory drugs: study in mitochondria, submitochondrial particles, cells, and whole heart. *Biochem. Pharmacol.* **1999**, *57* (7), 743–52.

(22) Mingatto, F. E.; Santos, A. C.; Uyemura, S. A.; Jordani, M. C.; Curti, C. In vitro interaction of nonsteroidal anti-inflammatory drugs on oxidative phosphorylation of rat kidney mitochondria: respiration and ATP synthesis. *Arch. Biochem. Biophys.* **1996**, *334* (2), 303–8.

(23) Masubuchi, Y.; Yamada, S.; Horie, T. Diphenylamine as an important structure of nonsteroidal anti-inflammatory drugs to uncouple mitochondrial oxidative phosphorylation. *Biochem. Pharmacol.* **1999**, *58* (5), 861–5.

(24) Mahmud, T.; Rafi, S. S.; Scott, D. L.; Wrigglesworth, J. M.; Bjarnason, I. Nonsteroidal antiinflammatory drugs and uncoupling of mitochondrial oxidative phosphorylation. *Arthritis Rheum.* **1996**, *39* (12), 1998–2003.

(25) Tomoda, T.; Kurashige, T.; Hayashi, Y.; Enzan, H. Primary changes in liver damage by aspirin in rats. *Acta Paediatr. Jpn.* **1998**, *40* (6), 593–6.

(26) Somasundaram, S.; Rafi, S.; Hayllar, J.; Sigthorsson, G.; Jacob, M.; Price, A. B.; Macpherson, A.; Mahmod, T.; Scott, D.; Wrigglesworth, J. M.; Bjarnason, I. Mitochondrial damage: a possible mechanism of the "topical" phase of NSAID induced injury to the rat intestine. *Gut* **1997**, *41* (3), 344–53.

(27) Hasebe, T.; Harasawa, S.; Miwa, T.; Shibata, T.; Inayama, S. Collagen and collagenase in ulcer tissue–1. The healing process of acetic acid ulcers in rats. *Tokai J. Exp. Clin. Med.* **1987**, *12* (3), 147–58.

in vivo *26*: 1015-1020 (2012)

Pilot Study of Changes in Salivary Metabolic Profiles Induced by Template Therapy

SHOJI TANAKA[1], HITOSHI TAGA[2], KIYOSHI MAEHARA[1], AZUSA KANESHIMA[1*], MAMORU MACHINO[1], HIROMI ONUMA[3], MIKU KANEKO[3], HIROSHI SAKAGAMI[1], MASAHIRO SUGIMOTO[3,4], TOMOYOSHI SOGA[3] and MASARU TOMITA[3]

[1]*Meikai University School of Dentistry, Sakado, Japan;*
[2]*JR Tokyo General Hospital, Shibuya-ku, Tokyo, Japan;*
[3]*Institute for Advanced Biosciences, Keio University, Tsuruoka, Yamagata, Japan;*
[4]*Graduate School of Medicine and Faculty of Medicine, Kyoto University, Sakyo-ku, Kyoto, Japan*
**Undergraduate student, Meikai University School of Dentistry*

Abstract. *Background: Occlusal raising method (so-called 'Template therapy') has been reported to alleviate various diseases and symptoms, but the underlying mechanism is not clear. We searched the low-molecular weight metabolite(s) in the saliva, the concentration of which is significantly changed by the template therapy. Materials and Methods: One female patient with headache underwent the template therapy for 12 days, and her total saliva was subjected to non-targeted analysis using capillary electrophoresis time-of-flight mass spectrometry (CE-TOF-MS). Results: One hundred and thirteen substances were identified in the saliva. Glycine was the most abundant amino acid in the saliva, followed by alanine, serine and proline. After the start of the template therapy, her headache was alleviated, accompanied by a significant ($p=0.042$) increase of salivary concentration of glycine, as compared with total amino acids whereas that of other amino acids was not significantly changed. In the metabolomics profile, salivary concentration of large number of metabolites as compared with total metabolite concentration decreased, including N-acetylneuraminate ($p=0.025$) and p-hydroxyphenylacetate ($p=0.039$). Conclusion: This pilot study demonstrated, to our knowledge for the first time, that only glycine exhibited unique changes among total metabolites, suggesting its significant role in template therapy.*

Correspondence to: Shoji Tanaka, Division of Oral Diagnosis, Department of Diagnostic and Therapeutic Sciences, Meikai University School of Dentistry, 1-1 Keyakidai, Sakado, Saitama 350-0283, Japan. Tel: +81 492792758, Fax: +81 492855511, e-mail: stanaka@dent.meikai.ac.jp

Key Words: Template therapy, metabolite profiling, salivary glycine.

There have been many clinical reports of various systemic symptoms such as headache, shoulder stiffness and mal-posture due to changes in the occlusal position (1-3). Several reports have attributed the artificial occlusal abnormalities to tooth extraction, bite raising and tooth grinding in experimental animals (4-9). These studies suggest that the trigeminal responses to occlusal changes induce various systemic symptoms by as yet -unidentified mechanisms. Out of these symptoms, the head drop and the drooping of the submandibular mental area to the ground were observed about one week after grinding the maxillary posterior teeth of guinea pigs to the cervical area. Abnormal waveforms including T-wave inversion were also observed on electrocardiogram (ECG) (9). We have recently reported that the decrease of the occlusal vertical dimension (OVD) in guinea pig models resulted in two-phase wave of heart rate fluctuations, with the first peak occurring 0-2 days after tooth grinding and the second peak starting from 4 days after teeth grinding until sudden death (usually 12th day), accompanied by the head drop, and that when the OVD was increased, such heart rate fluctuations disappeared (10). Although the occlusal raising method (the so-called 'Template therapy') has been reported to improve such systemic symptoms, the fundamental mechanism is not clear. In order to identify the biomarkers of compounds responsible for the efficacy of template therapy, we searched for low-molecular weight metabolites in the saliva, the concentration of which is significantly changed by template therapy, using capillary electrophoresis time-of-flight mass spectrometry (CE-TOF-MS).

Materials and Methods

Sample collection. A female patient (30 years old) had headache or tension-type headache, low back pain and shoulder stiffness, and had a medical examination in Maehara Dental Clinic, Shinjuku-

branch, Tokyo. She wore the template there on August 6, 2011 during her summer-time holiday, as previously reported (1). She used the template during sleeping and 2 h exercise for over 3 months. Her symptoms such as non-specific complaints, had disappeared after a week. Whole saliva (2-5 ml) was collected in a 50 ml centrifugation tube and immediately frozen at –20°C six times at 15, 14, 12, 10, 8, 4 days before the therapy and six times at 1, 3, 8, 14, 18, 22 days after the therapy. The CE-TOF-MS analysis of the collected saliva has been performed, according to the Guideline of the Intramural Ethics Committee (approved as no. A1113), as described below.

Sample preparation. Saliva was thawed and centrifugally-filtered through a 5-kDa cut-off filter (Millipore, Bedford, MA, USA) at 9,100 ×*g* for at least 2.5 h at 4°C to remove macromolecules. Five microliters of Milli-Q water containing internal standards (2 mmol/l each of methionine sulfone, 2-[*N*-morpholino]-ethanesulfonic acid, D-camphor-10-sulfonic acid, 3-aminopyrrolidine, and trimesate) was added to 45 μl of the filtrate and mixed immediately before CE-TOF-MS analysis.

CE-TOF-MS analysis. The instrumentation and measurement conditions used for CE-TOF-MS are described elsewhere (12, 13) with slight modifications. Briefly, cation analysis was performed using an Agilent CE capillary electrophoresis system, an Agilent G6220A LC/MSD TOF system, an Agilent 1100 series isocratic HPLC pump, a G1603A Agilent CE-MS adapter kit, and a G1607A Agilent CE-ESI-MS sprayer kit (Agilent Technologies, Waldbronn, Germany). Anion analysis was performed using an Agilent CE capillary electrophoresis system, an Agilent G6210A LC/MSD TOF system, an Agilent 1200 series isocratic HPLC pump, a G1603A Agilent CE-MS adapter kit, and a G1607A Agilent CE-electrospray ionization (ESI) source-MS sprayer kit (Agilent Technologies). For the cation and anion analyses, the CE-MS adapter kit includes a capillary cassette that facilitates thermostatic control of the capillary. The CE-ESI-MS sprayer kit simplifies coupling of the CE system with the MS system, and is equipped with an electrospray source. For system control and data acquisition, we used G2201AA Agilent ChemStation software for CE and the Agilent MassHunter software for TOF-MS. The original Agilent SST316Ti stainless steel ESI needle was replaced with a passivated SST316Ti stainless steel and platinum needle (passivated with 1% formic acid and 20% aqueous solution of isopropanol at 80°C for 30 min) for anion analysis.

For cationic metabolite analysis using CE-TOF-MS (12), sample separation was performed in fused silica capillaries (50 μm i.d. × 100 cm total length) filled with 1 mol/l formic acid as the reference electrolyte. Sample solutions (3 nl) were injected at 50 mbar for 5 s and a voltage of 30 kV was applied. The capillary temperature was maintained at 20°C and the temperature of the sample tray was kept below 5°C. The sheath liquid, composed of methanol/water (50% v/v) and 0.1 μmol/l hexakis(2,2-difluoroethoxy) phosphazene (Hexakis), was delivered at 10 μl/min. ESI-TOF-MS was conducted in the positive ion mode. The capillary voltage was set at 4 kV and the flow rate of nitrogen gas (heater temperature=300°C) was set at 7 psig. In TOF-MS, the fragmentor, skimmer and OCT RF voltages were 75, 50 and 125 V, respectively. Automatic recalibration of each acquired spectrum was performed using reference standards {[^{13}C isotopic ion of protonated methanol dimer (2MeOH+H)]$^+$, *m/z* 66.0632)} and {[protonated Hexakis (M+H)]$^+$, *m/z* 622.0290]}. Mass spectra were acquired at the rate of 1.5 cycles/s over a *m/z* range of 50-1,000.

For anionic metabolite analysis using CE-TOF-MS (14), a commercially available COSMO(+) capillary (50 μm i.d. × 105 cm, Nacalai Tesque, Kyoto, Japan), chemically-coated with a cationic polymer, was used for separation. Ammonium acetate solution (50 mmol/l; pH 8.5) was used as the electrolyte for separation. Before the first use, the new capillary was flushed successively with the running electrolyte (pH 8.5), 50 mmol/l acetic acid (pH 3.4), and then the electrolyte again for 10 min each. Before each injection, the capillary was equilibrated for 2 min by flushing with 50 mM acetic acid (pH 3.4) and then flushed for 5 min with the running electrolyte. A sample solution (30 nl) was injected at 50 mbar for 30 s, and a voltage of –30 kV was applied. The capillary temperature was maintained at 20°C and the sample tray was cooled below 5°C. An Agilent 1100 series pump, equipped with a 1:100 splitter was used to deliver 10 μl/min of 5 mM ammonium acetate in 50% (v/v) methanol/water, containing 0.1 μM Hexakis, to the CE interface. Here, it was used as a sheath liquid surrounding the CE capillary to provide a stable electrical connection between the tip of the capillary and the grounded electrospray needle. ESI-TOF-MS was conducted in the negative ionization mode at a capillary voltage of 3.5 kV. For TOF-MS, the fragmentor, skimmer and OCT RF voltages were set at 100, 50 and 200 V, respectively. The flow rate of the drying nitrogen gas (heater temperature=300°C) was maintained at 7 psig. Automatic recalibration of each acquired spectrum was performed using reference standards {[^{13}C isotopic ion of de-protonated acetic acid dimer (2 CH_3COOH-H)]$^-$, *m/z* 120.03841}, and {[Hexakis+ deprotonated acetic acid (M+CH_3COOH-H)]$^-$, *m/z* 680.03554}. Exact mass data were acquired at a rate of 1.5 spectra/s over a *m/z* range of 50-1,000.

Data analysis and statistical analysis. Raw data were analyzed by our proprietary software MasterHands (13), which follows typical data processing flows including detecting all possible peaks, eliminating noise and redundant features, and generating the aligned data matrix with annotated metabolite identities and relative area (peak areas normalized by those of internal standards) (15). Concentrations were calculated using external standards based on relative area. To eliminate the variation of overall concentration, the concentration of each metabolite was divided by the concentration of total metabolites (relative concentration), or that of each amino acid was divided by the concentration of total amino acids. Only the metabolites frequently observed in four, or more, out of six samples before or after template therapy were used for the data analysis. The student's *t*-test (two-tailed) was used for statistical comparisons.

Results

In total, 113 substances were identified in the saliva and, out of these, 56 metabolites frequently observed were used for the data analysis. Glycine was the most abundant amino acid in the saliva, followed by proline, alanine and serine (Figure 1A). After the start of the template therapy, the patient's headache was alleviated, accompanied by significant (p=0.042) increase of the salivary concentration of glycine, as compared with total amino acids whereas that of other amino acids was not significantly changed (Figure 1B).

After template therapy, the concentration of only six metabolites was increased [fold-change (FC) >1.2), out of which priopinate and urea were the most dominant, and the

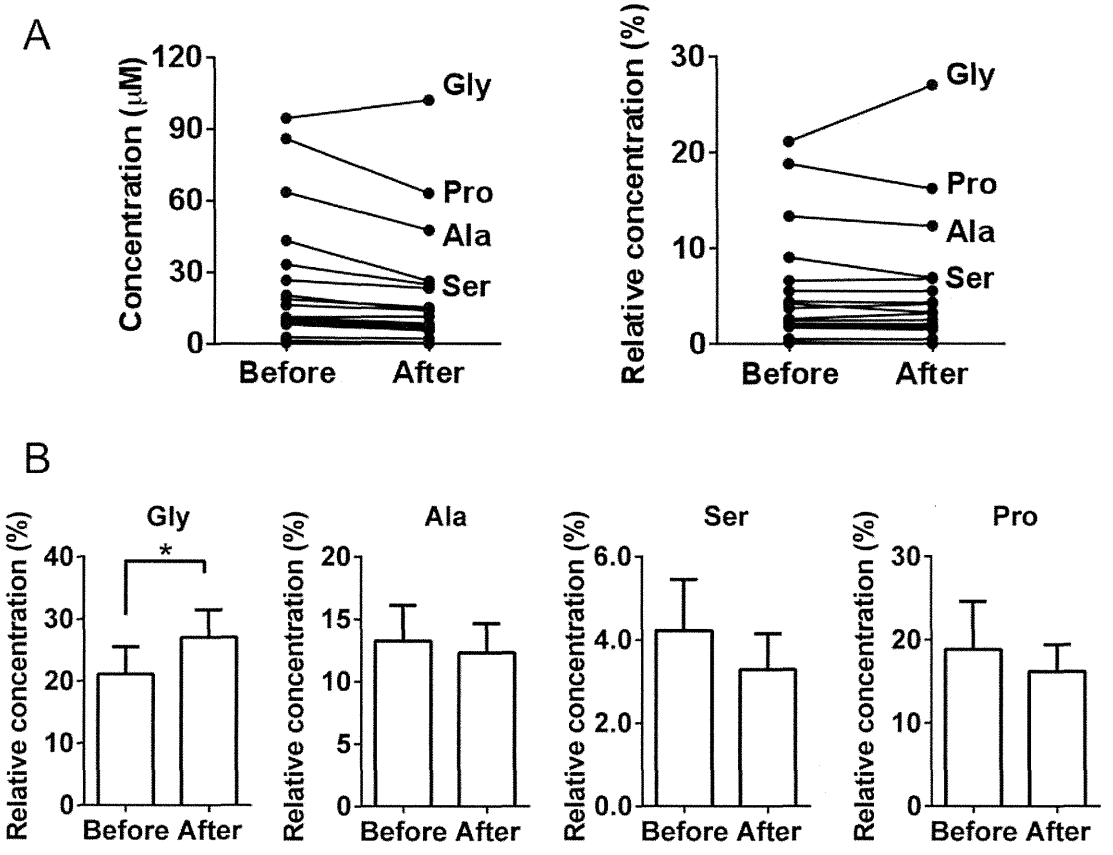

Figure 1. *Salivary amino acid concentrations before and after template therapy. A: Absolute concentration (left) and ratio of each amino acid to total amino acids (relative concentration) (right). B: Bar graph showing mean and standard deviation of the relative concentration of four major salivary amino acids, glycine, proline, alanine and serine. *p<0.05.*

relative concentrations of other metabolites were less than 1% (Figure 2A). No metabolite significantly increased in concentration. The concentration of many metabolites decreased after the therapy (FC<0.7), where *N*-acetylneuraminate (p=0.025) and *p*-hydroxyphenylacetate (p=0.039) was presented significantly decreased (Figure 2B). Out of these, 11 amino acids, namely proline, alanine, glutamate, glutamine, serine, asparagine, valine, phenylalanine, leucine, threonine and isoleucine, tended to decrease although not significantly. The other 23 metabolites, such as lactate and pyruvate, were hardly changed (data not shown).

Discussion

There are numerous reports that investigated the salivary concentration of amino acids in relation to caries (16, 17), periodontal diseases (18-20), phenylketonuria (21), migraine (22), a lacto-ovo vegetarian diet (23), smoking and gender difference (24), diurinal changes and aging (25). However, to our knowledge, none of these reports, except for ours (26), has attributed attention to the salivary glycine level. We reported that (i) glycine was the most abundant amino acid in the saliva; (ii) glycine and lysine concentrations increased significantly (p<0.05) with aging, regardless of gender difference; and (iii) glycine and lysine were positively correlated (p<0.001), (iv) however, there was no significant correlation between the salivary concentration of glutamic acid or histidine and age, suggesting that salivary amino acid levels may be regarded as markers of aging (26). The present study demonstrated that glycine was also the most abundant amino acid in the saliva of the female patient presented here, and glycine is the only amino acid that increased significantly with template therapy (Figure 1). This does not necessarily mean that the elevation of glycine is the result of accelerating the aging process, since the observed glycine concentration (at most 100 μM) is much smaller than the value reported in aged people (570 μM) (26). It is interesting to note that the plasma concentration of glycine is significantly reduced by occlusal destruction, producing the opposite effect to template therapy (27).

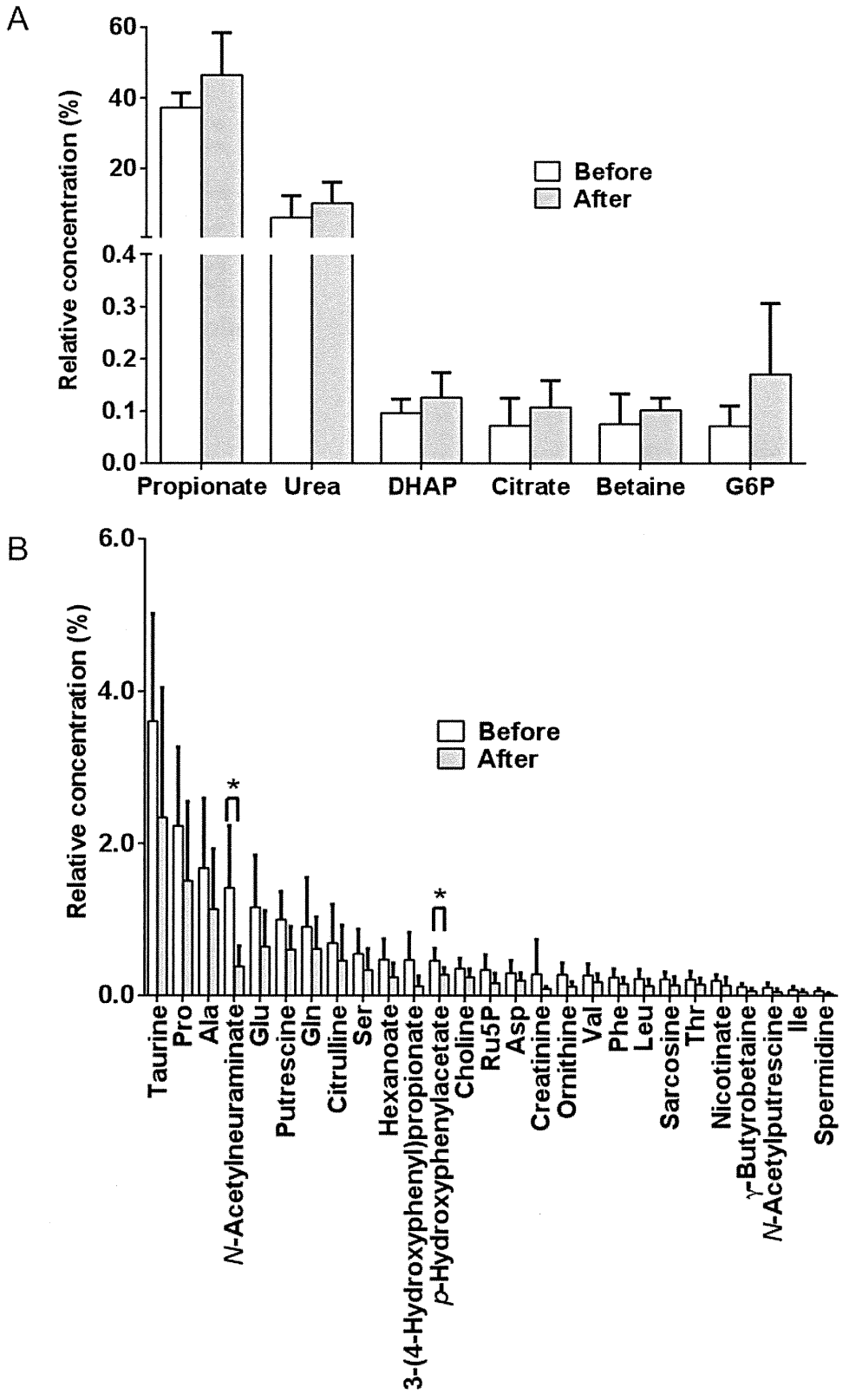

Figure 2. *Relative concentrations of metabolites before and after the template therapy. Metabolites increased (fold-change (FC) >1.2) (A) and reduced (FC<0.7) (B) after template therapy. Bar graph indicates mean and standard deviation. *p<0.05.*

The biological significance of the increase of the relative concentration of glycine by template therapy is unclear. Recent reports have suggested the possible role of glycine in inflammation. Glycine stimulated production of pro-inflammatory substances such as nitric oxide, prostaglandin E_2, tumor necrosis factor-α and cyclooxygenase-2 in macrophages, gingival fibroblasts and microglia (28-30). On the other hand, glycine exerts anti-inflammatory activity *via* glycine-activated chloride channels that suppress the production of oxidants and pro-inflammatory cytokines (31) and protected the cells from cadmium (32), cyclosporine-induced kidney damage (33) and liver injury (34, 35), suggesting a possible role of glycine in cell survival and activation. These data suggest dual actions of glycine.

In the metabolomics profiles, a large number of metabolites decreased in concentration (n=27) while that of a few metabolites increased (n=6) on template therapy. The decreased metabolites included many compounds related to nervous systems status; taurine was the most abundant and this metabolite acts as an inhibitory neurotransmitter and is used to aid the treatment of epilepsy and excitable brain status (36). Glutamine and asparagine are excitatory neurotransmitters within the central nervous system responsible for normal synaptic neurotransmission, serine acts as both neurotransmitter and neuromodulator, and alanine is also a neurotransmitter in the visual system (36). Only *N*-acetylneuraminate and *p*-phydroxyphenylacetate showed significant reduction (p=0.025 and p=0.039, respectively) after template therapy. *N*-Acetylneuraminate is the most prominent sialic acid that is a terminal sugar and acts as a marker for chronic inflammation in various systemic diseases, such as heart diseases (37, 38) and breast cancer (39). *p*-Hydroxyphenylacetate is expected to be produced by oral bacteria (40). Thus, the significant decrease of these salivary components might reflect the metabolic change of both systemic and oral physiological conditions. Further extensive studies with more patients are required to elucidate the biological significance of the present findings.

Acknowledgements

This work was supported by research funds from the Yamagata Prefectural Government and the City of Tsuruoka, and in part by a Grant-in-Aid for Scientific Research (C) of the Ministry of Education, Culture, Sports, Science and Technology of Japan (S. Tanaka, no. 24593164).

References

1 Maehara K, Tsuruhara T, Hase Y, Fukuda Y, Sawada Y, Yamamoto Y, Nakamura S, Takesada M, Nakajima A, Ito H, Matsui T, Takada F, Ueda T, Guzay C and Sato S: A template therapy approach for non-specific complaints. Basal Facts *8*: 22-35, 1986.

2 Nobili A and Adversi R: Relationship between posture and occlusion; A clinical and experimental investigation. J Craniomandib Pract *14*: 274-285, 1996.

3 Milani RS, de Periere DD and Micallef J-P: Relationship between dental occlusion and visual focusing. J Craniomandib Pract *16*: 109-118, 1998.

4 Tokita K, Ito R, Kawamura H, Sato Y, Terada K, Yamada M and Henomatsu H: Studies on teeth extraction phenomena. Comparative studies on electrocardiographic and histologic findings in rats, mice, hamsters and guinea-pigs. J Am College Cardiol *24*: 975-976, 1960.

5 Abe K, Yokota Y, Kawazoe T, Hioki S, Kishimoto T and Dawes C: The effects of an incisal bite plane on rat submandibular gland. J Dent Res *62*: 721-724, 1983.

6 Hioki S, Niwa K, Kishimoto T, Kawazoe T, Yokota Y, Abe K and Dawes C: The effects of an incisal bite plane on rat sublingual glands. J Dent Res *62*: 715-721, 1983.

7 Ueda T: Effects of occlusal destruction on posture in rats. J Gifu Dent Soc *18*: 192-202, 1991 (in Japanese).

8 Sumioka T: Systemic effects of the peripheral disturbance of the trigeminal system. Influence of the occlusal destruction in dogs. J Kyoto Pref Univ Med *98*: 1077-1085, 1991.

9 Azuma Y, Maehara K, Tokunaga T, Hashimoto M, Ieoka K and Sakagami H: Systemic effects of the occlusal destruction in guinea pigs. In Vivo *13*: 519-524, 1999.

10 Taga H, Azuma Y, Maehara K and Nomura S: Effects of changes in occlusal vertical dimension on heart rate fluctuations in guinea pigs. In Vivo *28*: 177-182, 2012

11 Soga T, Baran R, Suematsu M, Ueno Y, Ikeda S, Sakurakawa T, Kakazu Y, Ishikawa T, Robert M, Nishioka T and Tomita M: Differential metabolomics reveals ophthalmic acid as an oxidative stress biomarker indicating hepatic glutathione consumption. J Biol Chem *281*: 16768-16776, 2006.

12 Sugimoto M, Wong DT, Hirayama A, Soga T and Tomita M: Capillary electrophoresis mass spectrometry-based saliva metabolomics identified oral, breast and pancreatic cancer-specific profiles. Metabolomics *6*: 78-95, 2010.

13 Soga T, Igarashi K, Ito C, Mizobuchi K, Zimmermann HP and Tomita M: Metabolomic profiling of anionic metabolites by capillary electrophoresis mass spectrometry. Analytical chemistry *81*: 6165-6174, 2009.

14 Sugimoto M, Kawakami M, Robert M, Soga T and Tomita M: Bioinformatics tools for mass spectroscopy-based metabolomic data processing and analysis. Curr Bioinform *7*: 96-108, 2012.

15 Van Wuyckhuyse BC, Perinpanayagam HER, Bevacqua D, Raubertas RFm Billings RJ, Bowen WH and Tabak LA: Association of free arginine and lysine concentrations in human parotid saliva with caries experience. J Dent Res *74*: 686-690, 1995.

16 Fonteles CSR, Guerra MH, Ribeiro TR, Mendonça DN, de Carualho CBM, Monteiro AJ, Toyama DO, Toyama MH and Fonteles MC: Association of free amino acids with caries experience and *mutans streptococci* levels in whole saliva of children with early childhood caries. Arch Oral Biol *54*: 80-85, 2009.

17 Syrjänen S, Piironen P and Markkanen H: Free amino acid composition of wax-stimulated whole saliva in human subjects with healthy periodontium, severe chronic periodontitis and post-juvenile periodontitis. Arch Oral Biol *29*: 735-738, 1984.

18 Syrjänen S, Piironen P and Markkanen H: Free amino acid content of wax-stimulated human whole saliva as related to periodontal disease. Arch Oral Biol *32*: 607-610, 1987.

19 Syrjänen SM, Alakuijala P, Markkanen SO and Markkanen H: Free amino acid levels in oral fluids of normal subjects and patients with periodontal disease. Arch Oral Biol *35*: 189-193, 1990.
20 Liappis N, Pohl B, Weber HP and el-Karkani H: Free amino acids in saliva of children with phenylketonuria. Klin Padiatr *198*: 25-28,1986.
21 Rajda C, Tajti J, Komoróczy R, Seres E, Klivényi P and Vécsei L: Amino acids in the saliva of patients with migraine. Headache *39*: 644-649, 1999.
22 Linkosalo E, Markkanen H and Syrjanen S: Effects of a lacto-ovo vegetarian diet on the free amino acid composition of wax-stimulated whole human saliva. J Nutr *115*: 588-592, 1985.
23 Takeda I, Stretch C, Barnaby P, Bhatnager K, Rankin K, Fu H, Weljie A, Jha N and Slupsky C: Understanding the human salivary metabolome. NMR Biomed *22*: 577-584, 2009.
24 Bertram HC, Eggers N and Eller N: Potential of human saliva for nuclear magnetic resonance-based metabolomics and for health-related biomarker identification. Anal Chem *81*: 9188-9193, 2009.
25 Tanaka S, Machino M, Akita S, Yokote Y and Sakagami H: Changes in salivary amino acid composition during aging. In Vivo *24*: 853-856, 2010.
26 Maehara K, Taga H, Takayama F and Sakagami H: Biochemical Analysis of Occlusal Destruction. 48th Japanese Association for Oral Biology, Tsurumi, Kanagawa, Japan, 2006 abstract poster no. 374.
27 Carmans S, Hendriks JJ, Thewissen K, Van den Eynden J, Stinissen P, Rigo JM and Hellings N: The inhibitory neurotransmitter glycine modulates macrophage activity by activation of neutral amino acid transporters. J Neurosci Res *88*: 2420-2430, 2010.
28 Rausch-Fan X, Ulm C, Jensen-Jarolim E, Shcedle A, Boltz-Nitulescu G, Rausch WD and Matejka M: Interleukin-1β-induced prostaglandin E2 production by human gingival fibroblasts is up-regulated by glycine. J Periodontol *76*: 1182-1188, 2005.
29 Tanaka J, Toku K, Matsuda S, Sudo S, Fujita H, Sakanaka M and Maeda N: Induction of resting microglia in culture medium devoid of glycine and serine. Glia *24*: 198-215, 1998.
30 McCarty MF, Barroso-Aranda J and Contreras F: The hyperpolarizing impact of glycine on endothelial cells may be anti-atherogenic. Med Hypotheses *73*: 263-264, 2009.
31 Okoto T and Awhin EP: Glycine reduces cadmium-induced alterations in the viability and activation of macrophage U937 cells. Food Chem Toxicol *48*: 536-538, 2010.
32 Thurman RG, Zhong Z, von Frankenberg M, Stachlewitz RF and Bunzendahl H: Prevention of cyclosporine-induced nephrotoxicity with dietary glycine. Transplantation *63*: 1661-1667, 1997.
33 Benko T, Freda S, Gu Y, Best J, Baba HA, Schlaak JF, de Groot H, Fandrey J and Rauen U: Glycine pretreatment ameliorates liver injury after partial hepatectomy in the rat. J Invest Surg *23*: 12-20, 2010.
34 You HB, Wang Q, Li XH, Chen XF, Liu Zj and Gong JP: The protection mechanisms of glycine against liver injury induced by lipopolysaccharides. Zhonghua Gan Zang Bing Za Zhi *14*: 574-577, 2006 (in Chinese).
35 Zinellu A, Sotgia S, Pisanu E, Scanu B, Sanna M, Usai MF, Chessa R, Deiana L and Carru C: Quantification of neurotransmitter amino acids by capillary electrophoresis laser-induced fluorescence detection in biological fluids. Anal Bioanal Chem *398*: 1973-1978, 2010.
36 Hegde AM, Kavita R, Sushma KS and Suchetha S: Salivary sialic acid levels and dental health in children with congenital heart disease. J Clin Pediatr Dent *36*: 293-296, 2012.
37 Oktay S, Basar I, Emekli-Alturfan E, Malali E, Elemek E, Ayan F, Koldas L, Noyan U and Emekli N: Serum and saliva sialic acid in periodontitis patients with and without cardiovascular disease. Pathophysiol Haemost Thromb *37*: 67-71, 2010.
38 Ozturk LK, Emekli-Alturfan E, Kasikci E, Demir G and Yarat A: Salivary total sialic acid levels increase in breast cancer patients: A preliminary study. Med Chem *7*: 443-447, 2011.
39 O'Connor KE, Witholt B and Duetz W: p-Hydroxyphenylacetic acid metabolism in Pseudomonas putida F6. J Bacteriol *183*: 928-933, 2001.

Received September 10, 2012
Revised October 16, 2012
Accepted October 17, 2012

Analyst

Cite this: *Analyst*, 2012, **137**, 5026

www.rsc.org/analyst

PAPER

Sheathless capillary electrophoresis-mass spectrometry with a high-sensitivity porous sprayer for cationic metabolome analysis

Akiyoshi Hirayama, Masaru Tomita and Tomoyoshi Soga*

Received 12th April 2012, Accepted 8th September 2012
DOI: 10.1039/c2an35492f

Sheath-flow capillary electrophoresis-mass spectrometry (CE-MS) has emerged as a new tool for comprehensive analysis of charged metabolites. However, it needs to be more sensitive. Here, we report a sheathless capillary electrophoresis-electrospray ionization-mass spectrometry method for cationic metabolome analysis. This system used a high-sensitivity porous sprayer interface and 10% (v/v) acetic acid as the background electrolyte (BGE). Under optimized conditions, 53 cationic metabolites, including amino acids and their derivatives, amines, nucleic acids and small peptides, were successfully separated and selectively detected with a time-of-flight mass spectrometer. At a signal-to-noise ratio of three, the concentration detection limits for these compounds were between 0.004 and 0.8 μmol L^{-1} (amount detection limit, 0.01 to 2 fmol) with pressure injection at 20.7 kPa for 5 s (2.6 nL). Compared with conventional sheath-flow CE-MS, the detection limit of the present method was increased more than 5-fold for 21 (40%) of the compounds detected. When the method was applied to the analysis of cationic metabolites obtained from human urine, there was a 10-fold increase in the number of detected peaks compared with conventional methods. More than 180 successive runs could be conducted without any problems, and only the BGE needed to be changed.

Introduction

Metabolomics is the comprehensive analysis of endogenous small molecule metabolites (typically less than 1 kDa) in biological samples. Gas chromatography/mass spectrometry,[1,2] liquid chromatography-mass spectrometry,[3] or nuclear magnetic resonance spectroscopy[4] are commonly used for metabolomics. However, a standard metabolomics method has not been established. This is primarily because of the complexity, chemical diversity, and physical properties of the metabolome.[5] Recently, we have developed capillary electrophoresis-mass spectrometry (CE-MS) for metabolome analysis and successfully analyzed thousands of charged metabolites simultaneously.[6–12] The major advantages of CE-MS are its extremely high resolution, and that almost any charged species can be infused into the mass spectrometer.

Electrospray ionization (ESI) is a soft ionization technique that is suitable for mass measurement of species over a broad molecular mass range. ESI is commonly used for liquid chromatography-mass spectrometry and CE-MS analysis. However, in sheath-flow CE-MS, the ESI sprayer needs a sheath liquid to establish an electrical contact between the ends of the capillary and maintain stable electrospray. However, the main disadvantage of sheath-flow configurations is their low sensitivity because of dilution of the analyte by the sheath liquid.[13]

To improve sensitivity, various sheathless CE-MS interfaces have been developed. For example, the outer surface of the capillary has been coated with conductive materials such as gold,[14,15] silver,[16] copper,[17] or graphite,[18] which allow the electrical contact to be established. However, these coatings are often damaged by electrical discharge and this reduces the lifetime of the electrical contact. In another approach, a platinum wire was inserted into the capillary to establish a stable electric contact,[19] but this caused bubble formation in the capillary. A split-flow technique has been developed where a small hole or a locally porous section was made near the capillary outlet wall, and a small portion of the background electrolyte (BGE) exited through this hole/section and contacted with an external electrode *via* the BGE reservoir.[20,21] However, most of these techniques require special equipment and skilled operators, which limits their application.

Recently, Moini has introduced a novel sheathless interface consisting of a porous tip at the capillary, and the electrical connection was established through this tip.[22] To form the porous tip, a 3–4 cm section of the capillary outlet was etched with a solution of 49% hydrofluoric acid. The electrical contact between the porous capillary and the ESI was achieved by filling the ESI needle with a static conductive liquid.

Based on this concept, a prototype high-sensitivity porous sprayer (HSPS) sheathless interface for CE-MS has been recently

Institute for Advanced Biosciences, Keio University, Tsuruoka, Yamagata 997-0052, Japan. E-mail: soga@sfc.keio.ac.jp; Fax: +81-235-29-0574; Tel: +81-235-29-0528

developed by Beckman Coulter (Brea, CA). This HSPS has been used for the analysis of peptide mixtures,[23,24] intact proteins,[25] and phosphorus-containing amino acid-type herbicides.[26] Recently, Ramautar *et al.* have evaluated the performance of this interface for the analysis of 21 metabolites including amino acids and their derivatives in urine sample.[27] Nevertheless, the evaluation of HSPS sheathless interface on other physiologically important metabolites has yet to be demonstrated.

In this study, we developed a sheathless CE-MS method using the prototype HSPS capillary to analyze a wider range of cationic metabolites. We have selected 53 metabolites including amino acids and their derivatives, amines, nucleic acids and small peptides, which are metabolically important intermediates in amino acid anabolism/catabolism, purine/pyrimidine metabolism and glutathione biosynthesis, and therefore important for the understanding of the global metabolism in living systems. The sensitivities from the optimized method were compared with those from conventional sheath-flow CE-MS, and the developed method was applied to metabolome analysis of human urine.

Results and discussion

Development of sheathless CE-MS using a HSPS capillary

In sheathless CE-MS, the BGE composition and pH are important factors for controlling the peak resolution because these parameters affect the electroosmotic flow rate. We first tried 1 mol L^{-1} formic acid (pH 1.8) as the BGE, because it is often used in conventional sheath-flow CE-MS.[28] However, with formic acid, the current dropped several minutes after applying voltage, although the reason for this was unclear. To overcome this problem, we examined alternative BGEs and found that the drop in current did not occur with acetic acid. The effect of changing the acetic acid concentration (100 mmol L^{-1}, 850 mmol L^{-1}, and 1.7 mol L^{-1}) on the resolution of leucine and iso-leucine was investigated (Fig. 1). The two structural isomers, leucine and iso-leucine, were not separated using 100 mmol L^{-1} acetic acid, but were partially separated in 850 mmol L^{-1} (5% v/v) acetic acid, and good separation was achieved using

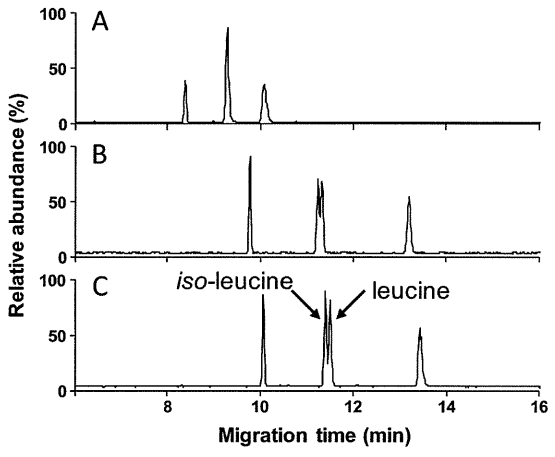

Fig. 1 Electropherograms for the separation of leucine and iso-leucine at three different BGE concentrations. (A) 100 mmol L^{-1} acetic acid; (B) 5% (v/v, 0.85 mol L^{-1}) acetic acid and (C) 10% (v/v, 1.7 mol L^{-1}) acetic acid.

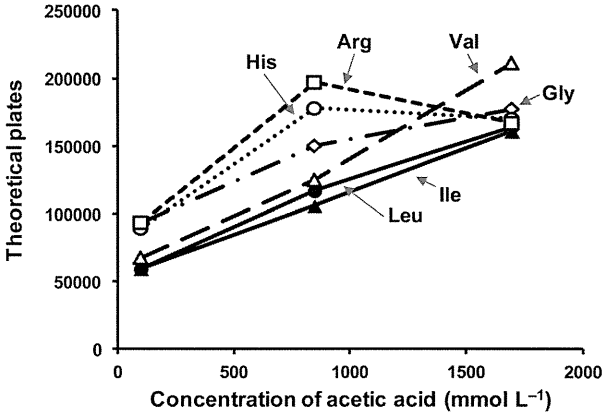

Fig. 2 Effect of acetic acid concentration on the number of theoretical plates for several amino acids.

1.7 mol L^{-1} (10% v/v) acetic acid. As reported previously,[28] at higher BGE concentrations, the number of theoretical plates for most amino acids increases (Fig. 2), so complete resolution of leucine and iso-leucine was obtained at 1.7 mol L^{-1}. The reason why the number of theoretical plates increases at higher BGE concentrations can be due to decreased interaction between the protonated analyte and capillary wall by ion exchange at lower pH. Next, the addition of methanol to the BGE was evaluated. Addition of organic solvents can reportedly reduce surface tension and provide stable spray formation,[29] and influence the signal intensity and migration times.[18] Fig. 3 depicts the changes in the signal-to-noise ratios of tryptophan, histidine and glycine with different methanol volume fractions in the BGE. The signal-to-noise ratio tended to decrease with the increase of the volume fraction of methanol, which indicates that the addition of methanol to the BGE decreases the signal intensity. These results are inconsistent with an earlier study,[18] in which the addition of methanol (volume fraction $\leq$ 30%) increased the signal intensity of hormones in a polyimide graphic coated sheathless CE-MS system. It should be noted that the analytical conditions were different from those used in the present study. In the previous report, the capillary had a relatively large i.d. (75 μm) and the BGE had a higher pH (2.85). These differences would lead to a higher BGE elution rate compared with the

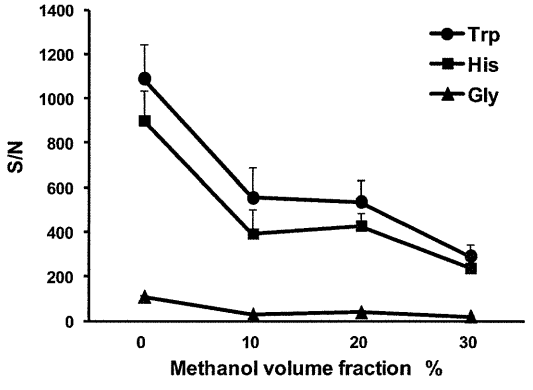

Fig. 3 Effect of addition of methanol to the BGE on the signal-to-noise ratio (*S/N*) of tryptophan (Trp), histidine (His) and glycine (Gly).

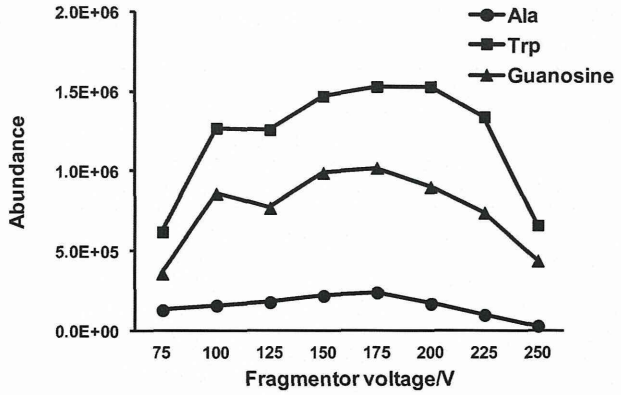

Fig. 4 Effect of the fragmentor voltage on the abundance of alanine (Ala, *m/z* 90.055), tryptophan (Trp, *m/z* 205.097) and guanosine (*m/z* 284.099).

present study, and we assume that the addition of organic solvent was necessary to stabilize the spray and obtain sufficient signal intensity in this study. Considering these observations, we selected 1.7 mol L^{-1} (10%) acetic acid without methanol as the BGE.

Optimization of the TOFMS parameters

In CE-TOFMS, the fragmentor voltage, skimmer voltage, and Oct RFV can affect sensitivity of the instrument. To optimize these parameters, a solution of three reference standards (alanine, *m/z* 90.055; tryptophan, *m/z* 205.097; guanosine, *m/z* 284.099) was infused electrokinetically by applying a CE voltage of 25 kV. Fig. 4 shows the signal intensities of the reference compounds, in which the fragmentor voltage was varied from 75 to 250 V.

At 75 V, the signal intensities of the three compounds were relatively small and there was a lot of background noise, especially at *m/z* <150. The signal intensities gradually increased as the fragmentor voltage increased, and reached their maximum values at 175 V. When the fragmentor voltage was set above 175 V, the intensities decreased, probably because of extensive fragmentation. However, in this study, we used a fragmentor

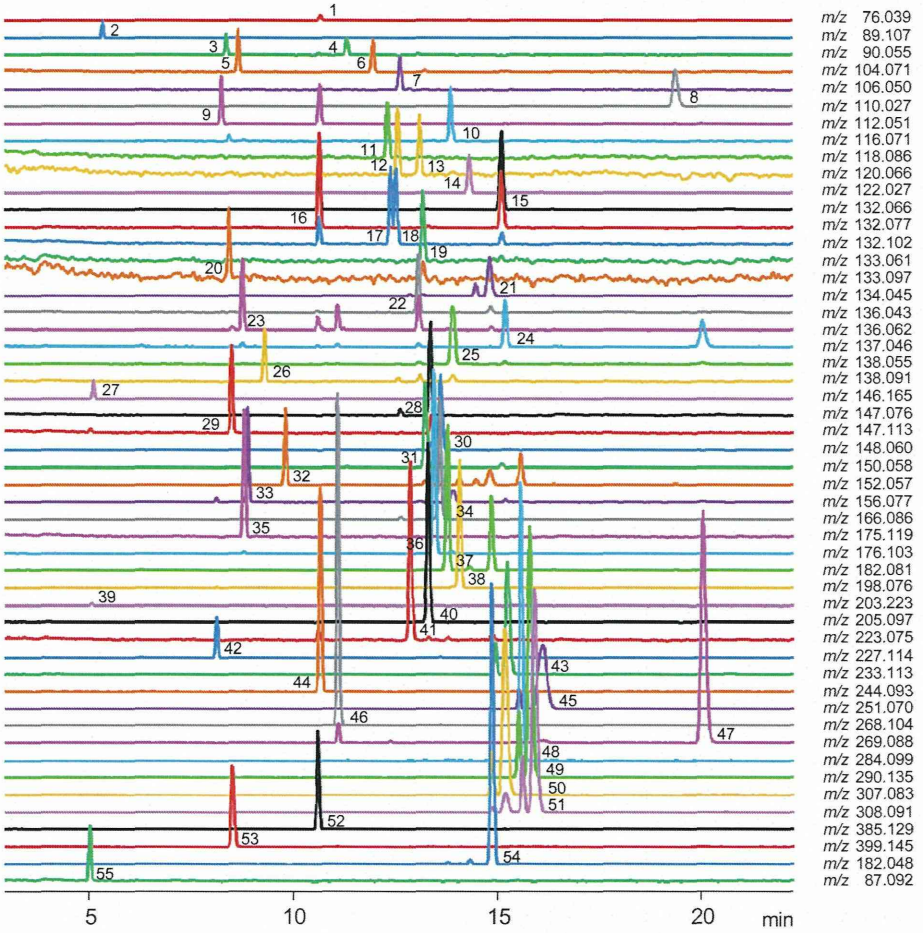

Fig. 5 Selected ion electropherograms for a standard mixture of 53 cationic metabolites obtained by sheathless CE-TOFMS. Peak identification: (1) Gly; (2) putrescine; (3) β-Ala; (4) Ala; (5) γ-aminobutyric acid; (6) 2-aminobutyric acid; (7) Ser; (8) hypotaurine; (9) cytosine; (10) Pro; (11) Val; (12) homoserine; (13) Thr; (14) Cys; (15) hydroxyproline; (16) creatine; (17) Ile; (18) Leu; (19) Asn; (20) ornithine; (21) Asp; (22) homocysteine; (23) adenine; (24) hypoxanthine; (25) anthranilate; (26) tyramine; (27) spermidine; (28) Gln; (29) Lys; (30) Glu; (31) Met; (32) guanine; (33) His; (34) Phe; (35) Arg; (36),citrulline; (37) Tyr; (38) 3,4-dihydroxyphenylalanine; (39) spermine; (40) Trp; (41) cystathionine; (42) carnosine; (43) γ-glutamyl-2-aminobutyrate; (44) cytidine; (45) γ-glutamylcysteine; (46) adenosine; (47) inosine; (48) guanosine; (49) ophthalmic acid; (50) oxidized glutathione; (51) reduced glutathione; (52) *S*-adenosylhomocysteine; (53) *S*-adenosylmethionine; (54) methionine sulfone (internal standard); (55) 3-aminopyrrolidine (internal standard). *Experimental conditions*: standard concentration, 10 μmol L^{-1} each; other experimental conditions are described in the Experimental section.

voltage of 200 V. This is because when the fragmentor voltage was set at 175 V, background noise was observed at *m/z* 82 and 105, but these interferences were considerably decreased at 200 V (data not shown). Most metabolites have molecular masses less than 300 Da, and a low background noise within this range is important for metabolome analysis.

Optimization of the skimmer voltage and Oct RFV was also investigated, but these parameters had a minimal effect on the signals of the reference compounds within the studied range. The optimized TOFMS parameters were as follows: fragmentor voltage, 200 V; skimmer voltage, 75 V; and Oct RFV, 250 V.

Method validation

Under the optimized conditions, we investigated the reproducibility, linearity and sensitivity of the sheathless CE-TOFMS method using 53 cationic metabolite standards, including amino acids and their derivatives, amines, nucleic acids and small peptides, which are predominant metabolites in biological samples. Extracted ion electropherograms of the 53 cationic metabolite standards were obtained by sheathless CE-TOFMS in positive mode using the HSPS capillary (Fig. 5). The monovalent protonated molecular $[M + H]^+$ ion peaks had the highest intensities for most of the compounds, except for oxidized glutathione, which had a higher intensity for divalent $[M + 2H]^{2+}$ than the monovalent ion.

The relative standard deviations were better than 1.4% for the migration times and between 2.4% and 18% for the normalized peak areas (Table 1). The calibration curves for all 53 cationic metabolite standards were linear with correlation coefficients between 0.9920 and 0.9999. The concentration detection limit for all species was between 0.004 and 0.8 μmol L^{-1}, which corresponds to a mass detection limit between 0.01 and 2 fmol, at a signal-to-noise ratio of three. These results indicate that the proposed method could be applied to simultaneous and quantitative analysis of cationic compounds.

Table 1 Reproducibility, linearity and sensitivity in the sheathless CE-TOFMS method

Compound	RSD (n = 10%) Migration time	Peak area	Relative peak area	Linearity correlation	Detection limit concentration (μmol L^{-1})
Gly	0.8	20	10	0.9987	0.3
Putrescine	0.7	18	14	0.9970	0.03
Ala	0.9	19	8.3	0.9987	0.2
β-Ala	0.7	18	11	0.9939	0.1
2-AB	0.9	17	6.3	0.9982	0.2
GABA	0.7	19	13	0.9992	0.1
Ser	1.0	18	6.0	0.9988	0.1
Hypotaurine	1.4	15	6.9	0.9955	0.07
Cytosine	0.7	14	6.7	0.9999	0.03
Pro	1.0	17	12	0.9993	0.08
Val	0.9	19	6.7	0.9988	0.5
Thr	0.9	18	5.4	0.9987	0.4
Homoserine	0.9	17	5.9	0.9993	0.4
Cys	1.0	19	10	0.9984	0.03
Hydroxy proline	1.1	14	6.2	0.9997	0.03
Creatine	0.8	21	10	0.9999	0.07
Ile	0.9	20	7.9	0.9994	0.2
Leu	0.9	19	9.5	0.9994	0.2
Asn	0.9	16	6.4	0.9991	0.8
Ornithine	0.7	19	16	0.9920	0.6
Asp	1.1	16	2.4	0.9957	0.09
Homocysteine	1.0	18	4.5	0.9998	0.07
Adenine	0.7	15	12	0.9994	0.04
Hypoxanthine	1.1	14	4.9	0.9993	0.2
Anthranilate	1.0	17	11	0.9965	0.03
Tyramine	0.7	14	8.5	0.9992	0.2
Spermidine	0.7	21	16	0.9944	0.03
Gln	1.0	16	4.7	0.9997	0.1
Lys	0.7	18	13	0.9997	0.09
Glu	1.0	15	4.7	0.9985	0.1
Met	1.0	18	6.2	0.9985	0.02
Guanine	0.8	13	8.4	0.9967	0.03
His	0.7	15	14	0.9986	0.03
Phe	1.0	17	6.1	0.9988	0.03
Arg	0.7	15	12	0.9998	0.06
Citrulline	1.0	14	6.1	0.9997	0.02
Tyr	1.0	13	5.3	0.9995	0.02
DOPA	1.0	13	6.6	0.9956	0.02
Spermine	0.5	22	18	0.9958	0.4
Trp	1.0	16	3.8	0.9995	0.03
Cystathionine	0.9	16	4.5	0.9992	0.07
Carnosine	0.7	17	13	0.9996	0.07
γ-Glu-2AB	1.0	14	5.3	0.9982	0.04
Cytidine	0.8	12	6.7	0.9996	0.004
γ-Glu-Cys	1.0	13	4.6	0.9961	0.05
Adenosine	0.8	11	6.0	0.9958	0.006
Inosine	1.4	12	13	0.9924	0.01
Guanosine	1.1	11	6.1	0.9982	0.004
Ophthalmate	1.1	11	6.1	0.9972	0.006
GSSG	1.1	14	4.4	0.9990	0.01
GSH	1.2	11	7.7	0.9992	0.007
SAH	0.8	19	9.4	0.9988	0.01
SAM	0.7	20	14	0.9984	0.008

Sensitivity comparison between sheath-flow and sheathless CE-TOFMS

To evaluate the sensitivity of the sheathless CE-TOFMS method, the detection limits of all species were compared among three different CE-TOFMS methods; sheath-flow CE-TOFMS with 1 mol L^{-1} formic acid, sheath-flow CE-TOFMS with 10% acetic acid, and sheathless CE-TOFMS with 10% acetic acid as BGE (Table 2). Compared with the conventional sheath-flow CE-TOFMS method with 1 mol L^{-1} formic acid, the detection limits of 21 (40%) of the compounds were at least five times better in sheathless CE-TOFMS. By contrast, the detection limits of asparagine, ornithine, tyramine and spermine decreased by half or more compared with conventional sheath-flow CE-TOFMS. Similar trends were observed between sheathless CE-TOFMS and sheath-flow CE-TOFMS methods with 10% acetic acid. The detection limits of 13 (25%) of the compounds were at least five times better in sheathless CE-TOFMS than in sheath-flow CE-TOFMS with 10% acetic acid. The detection limits of asparagine, ornithine, tyramine, spermidine and spermine were at least five times worse in the sheathless CE-TOFMS than in sheath-flow CE-TOFMS with 10% acetic acid. Decreased sensitivity in the sheathless CE-TOFMS was probably caused by high background noise. For example, the average baseline noise between 3 and 5 min in the selected ion electropherograms of asparagine in sheath-flow CE-TOFMS with 1 mol L^{-1} formic acid, sheath-flow CE-TOFMS with 10% acetic acid, and in the sheathless CE-TOFMS method was 454, 418 and 22 408, respectively. This indicates that asparagine would overlap with the high

Table 2 Sensitivity comparison among three different CE-TOFMS methods

Compound	HSPS_10% acetic acid		Sheath flow_10% acetic acid		Sheath flow_1 mol L^{-1} formic acid		Sensitivity comparison[a]	
	Detection limit concentration (μmol L^{-1})	Noise	Detection limit concentration (μmol L^{-1})	Noise	Detection limit concentration (μmol L^{-1})	Noise	HSPS *vs.* acetate	HSPS *vs.* formate
Gly	0.3	772	0.4	1604	0.7	1062	1.4	2.2
Putrescine	0.03	367	0.02	282	0.03	211	0.7	1.0
Ala	0.2	1952	0.2	818	0.4	801	0.9	1.9
β-Ala	0.1	1952	0.1	818	0.4	801	0.7	2.8
2-AB	0.2	2548	0.09	344	0.1	376	0.6	0.8
GABA	0.1	2548	0.04	344	0.1	376	0.4	1.1
Ser	0.1	2002	0.4	1287	0.8	1140	3.0	6.1
Hypotaurine	0.07	605	0.7	817	0.5	179	10.2	6.2
Cytosine	0.03	721	0.04	278	0.09	220	1.5	3.0
Pro	0.08	1815	0.2	544	0.2	532	2.1	2.9
Val	0.5	13 247	0.3	1366	0.4	1409	0.6	0.8
Thr	0.4	10 636	0.2	659	0.4	586	0.5	1.0
Homoserine	0.4	10 636	0.2	659	0.4	586	0.6	1.1
Cys	0.03	332	0.1	223	0.1	151	3.4	3.8
Hydroxyproline	0.03	785	0.1	223	0.2	241	3.7	6.2
Creatine	0.07	3429	0.05	223	0.08	208	0.7	1.1
Ile	0.2	5997	0.2	856	0.2	788	1.0	1.1
Leu	0.2	5997	0.2	856	0.2	779	0.9	1.0
Asn	0.8	22 408	0.1	418	0.3	454	0.2	0.4
Ornithine	0.6	20 033	0.1	879	0.3	864	0.2	0.4
Asp	0.09	1107	0.3	501	0.7	576	3.4	7.3
Homocysteine	0.07	1553	0.08	183	0.1	145	1.1	1.8
Adenine	0.04	1294	0.04	273	0.07	217	1.1	2.0
Hypoxanthine	0.2	2589	0.1	308	0.9	722	0.9	5.4
Anthranilate	0.03	729	0.07	218	0.09	198	2.3	2.9
Tyramine	0.2	4367	0.03	198	0.06	202	0.2	0.4
Spermidine	0.03	393	0.006	87	0.02	116	0.2	0.6
Gln	0.1	3908	0.2	464	0.3	527	1.6	3.1
Lys	0.09	3827	0.07	548	0.2	418	0.8	1.9
Glu	0.1	2549	0.2	503	0.3	525	1.7	3.3
Met	0.02	639	0.06	189	0.08	168	3.0	3.9
Guanine	0.03	929	0.05	257	0.2	326	1.6	5.7
His	0.03	1405	0.07	511	0.2	414	2.2	4.9
Phe	0.03	1283	0.1	451	0.1	406	4.3	5.1
Arg	0.06	3754	0.04	364	0.1	335	0.6	1.7
Citrulline	0.02	1131	0.06	227	0.2	222	3.7	10.3
Tyr	0.02	945	0.2	486	0.3	471	8.2	13.6
DOPA	0.02	587	0.1	242	0.1	177	4.8	5.6
Spermine	0.4	552	0.03	134	0.04	362	0.1	0.1
Trp	0.03	1583	0.1	357	0.1	232	3.4	3.8
Cystathionine	0.07	4255	0.8	2226	0.4	779	11.4	5.6
Carnosine	0.07	1706	0.09	274	0.1	400	1.2	1.3
γ-Glu-2AB	0.04	1101	0.2	340	0.2	189	6.5	4.7
Cytidine	0.004	309	0.03	169	0.08	80	7.2	18.2
γ-Glu-Cys	0.05	720	1.6	1257	1.7	1166	30.0	31.5
Adenosine	0.006	699	0.03	147	0.06	128	4.0	9.6
Inosine	0.01	596	0.2	228	0.4	195	19.6	31.7
Guanosine	0.004	285	0.05	112	0.06	78	13.8	15.5
Ophthalmate	0.006	324	0.08	177	0.1	136	14.6	18.0
GSSG	0.01	553	0.07	207	0.1	125	5.2	8.2
GSH	0.007	387	0.07	110	0.1	100	9.9	19.5
SAH	0.01	547	0.07	103	0.1	265	5.8	11.1
SAM	0.008	280	0.1	96	0.1	245	13.3	15.8

[a] Values were calculated by dividing the detection limit with both the sheath flow with 10% acetic acid and the sheath flow with 1 mol L^{-1} formic acid by that with the HSPS with 10% acetic acid.

background noise in sheathless CE-TOFMS, and this would decrease the sensitivity. The use of multiple reaction monitoring with triple quadrupole MS may improve the selectivity and reduce the high background noise.

Overall, about half of the 53 compounds tested showed increased sensitivity in the sheathless CE-TOFMS method compared with conventional methods. The sensitivity for several compounds, including γ-glutamylcysteine, inosine, guanosine, ophthalmic acid, reduced glutathione and *S*-adenosylmethionine, increased more than 10 times compared with both the sheath-flow methods. The *m/z* values of these compounds were above 250 where no significant background noise was observed, and this facilitated the increase in sensitivity in the sheathless method.

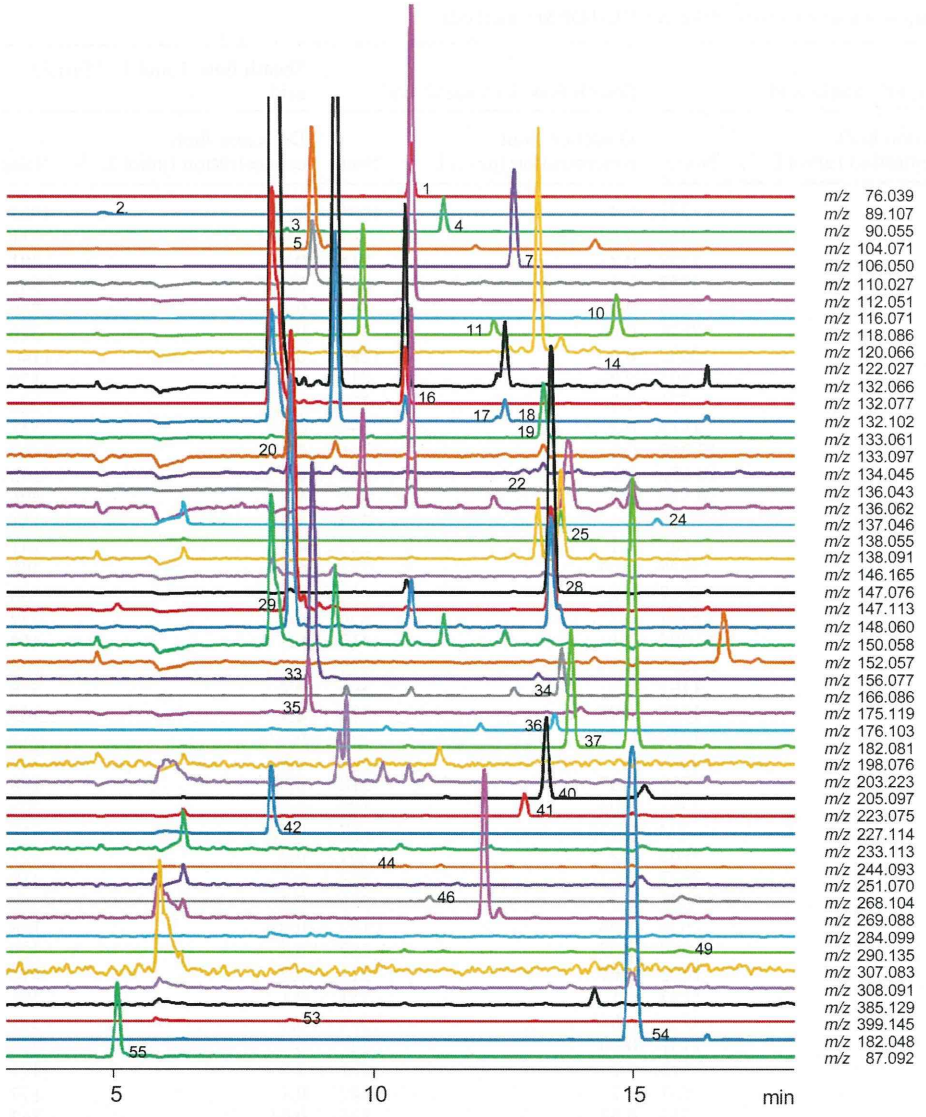

Fig. 6 Selected ion electropherograms of cationic metabolites in human urine. Peak identifications are the same as in Fig. 5. Experimental conditions are described in the Experimental section.

Application to metabolome analysis of human urine

The sheathless CE-TOFMS method was applied to metabolome analysis of human urine. Fig. 6 shows the selected ion electropherograms of 53 cationic compounds in human urine from a healthy volunteer that was analyzed by sheathless CE-TOFMS. The 31 compounds were identified by matching their molecular masses and migration times with those of standards. The number of peaks detected with sheath-flow CE-TOFMS with 1 mol L^{-1} formic acid and sheathless CE-TOFMS were compared. Setting a threshold value of a signal-to-noise of three, 1659 peaks were detected with the sheath-flow CE-TOFMS method, while 16 147 peaks were detected with sheathless CE-TOFMS on average (Table 3). The number of peaks detected in all signal-to-noise ratio categories for the sheathless method was more than seven times compared with the sheath-flow method. This indicates that the sheathless method is more effective than the sheath-flow method for the detection of small peaks. Finally, the robustness of the HSPS capillary was investigated. For over 180 successive analyses only a slight drop in the current and small fluctuations in the migration time were observed, and the capillary did not require any modifications except for changing the BGE. Overall, sheathless CE-MS provides a several-fold increase in sensitivity for compounds with *m/z* >250. If elimination of background noise in the region below *m/z* 250 is possible, this method could be a powerful tool for metabolome analysis.

Experimental

Chemicals

Methionine sulfone (internal standard) was purchased from Alfa Aesar (Ward Hill, MA), ophthalmate from Bachem (Bubendorf, Switzerland), hexakis-(2,2-difluorothoxy)-phosphazene (hexakis) from SynQuest Laboratories (Alachua, FL), and 2-aminobutyrate, hypotaurine, cytosine, homocysteine, hypoxanthine, cystathionine, *S*-adenosylhomocysteine and 3-aminopyrrolidine (reference compound) from Sigma-Aldrich (St Louis, MO).